JPRS-UEQ-89-010
22 JUNE 1989

JPRS Report

Science & Technology

USSR: Engineering & Equipment

DTIC QUALITY INSPECTED 2

19980506 089

Science & Technology
USSR: Engineering & Equipment

CONTENTS

Aviation and Space Technology

Optics, High Energy Devices

Nuclear Energy

Non-Nuclear Energy

Turbines, Engines, Propulsion Systems

Industrial Technology, Planning, Productivity

Abstracts From Journal MEKHANIKA GIROSKOPICHESKIKH SISTEM

Vol 4, 1985

81440686 Kiev MEKHANIKA GIROSKOPICHESKIKH SISTEM in Russian Vol 4, 1985 (signed to press 21 Nov 84) pp 123-127

[Abstracts of articles appearing in "Mechanics of Gyroscopic Systems," 1985]

[Text]

UDC 531.383

Equations of Motion of Multirace Tuned Rotor Gyroscopes. O. F. Boychuk, A. V. Zbrutskiy, and M. A. Pavlovskiy, p 3

The kinematics of multirace tuned rotor gyroscopes is studied and differential equations of motion that reflect the specifics of a flexible suspension are compiled. Conditions for matching the angles of rotation and the absence of "jamming" of the gyroscope rotor are found. 2 Tables, 1 figure, 1 reference.

UDC 681.2.082

Calculation of Stator Characteristic of Resonator of Rod Vibration Frequency Pickup. A. V. Bytsenko, Yu. A. Kravtsov, and N. M. Lokot, p 11

The static characteristic of a mechanical rod resonator is found with regard to the inertia of cross-sectional rotation and shearing strain with transverse vibrations of the rod. It is compared numerically to the characteristic calculated without regard to the indicated factors. 2 Figures, 3 references.

UDC 531:534.2

Natural Oscillations of Rotating Solid With Respect to Center of Mass in Central Force Field. V. I. Gulyayev, P. P. Lizunov, and V. A. Saushev, p 14

Nonlinear oscillations of a rotating solid are considered with respect to a center of mass moving along an angular trajectory in a central force field. Periodic solutions of the equations of motion are constructed by modifying the method of continuation of the solution with respect to the parameter. The amplitude-frequency characteristics are presented at different values of the inertial parameters of the body. The stability of the derived solutions is analyzed. 2 Figures, 5 references.

UDC 531.383

Effect of Practically Feasible Factors on Elastic Characteristics of Torsional Suspension of One-Axis Gyroscope. V. V. Demyanenko and V. M. Slyusar, p 19

The matrix of stiffnesses with regard to practically feasible errors of manufacture and assembly is found and analyzed for a flexible suspension of a one-axis gyroscope in the form of rods arranged along the precession axis. 3 References.

UDC 531.534

On Natural Oscillations of Gyromotors. V. S. Ditkovskiy, p 23

Natural oscillations of a gyromotor, represented in the form of two rectangular plates, are considered in the article. A concentrated mass is suspended on flexible connections between the plates. The oscillations of the system are studied with regard to Fourier methods and asymptotic methods of nonlinear mechanics. A solution is found for the single-frequency oscillation mode. 2 References.

UDC 531.383

Determination of Stiffness of Flexible Suspension of Tuned Rotor Gyroscope. A. V. Zbrutskiy and V. R. Maresh, p 29

The stiffness of the flexible suspension of a single-race tuned rotor gyroscope in three mutually perpendicular directions is determined. Functions that take into account the finite stiffness of the center ring are found. 2 Figures, 6 references.

UDC 531.383

Two-Channel Automatic Compensation of Drift of a Free Gyroscope Is Considered. V. V. Karachun, p 35

A two-channel layout for automatic compensation of the draft of a free gyroscope is considered. The effectiveness of the scheme at small arbitrary perturbations of the base is shown. 8 References.

UDC 532.516:531.383

Use of Finite Element Method To Calculate Flow of Slightly Compressible Liquid in Floated Suspension. A. S. Kiryeyev, p 38

The finite element postulation of the problem of dynamics of a viscous liquid in a floated suspension is presented on the basis of the maximum transition to the model of a slightly compressible flow. The results of calculation for two model examples are presented. The numerical and analytical solutions are compared. 2 Figures, 4 references.

UDC 531.383

Dynamics of Correctable Gyrocompass Upon Positive Vibration of Base. V. N. Koshlyakov, M. A. Pavlovskiy, and L. M. Ryzhkov, p 41

The dynamics of a single-rotor correctable gyrocompass with statically unbalanced sensitive element is considered. Expressions are found for errors upon positive vibration of the base. 2 References.

UDC 519.6

Algorithm for Constructing Numerical Analytical Solution of Averaged System of Differential Equations. O. P. Marosin and S. Ya. Svistunov, p 47

An algorithm is proposed for construction of the numerical analytical solution of an averaged system if differential equations, based on approximation of the solution by Fourier series and on an iteration procedure for determining the numerical coefficients of the expansion. 4 References.

UDC 621.396:629.7.062

On Use of Platformless Orientation System for Stabilization of the Radiation Pattern of a Direction Finder. V. V. Meleshko and V. A. Stepanov, p 50

Equations of stabilization of the radiation pattern of direction finders during use of a platformless orientation system are found. Angular rate meters are used as its sensitive elements. A method is proposed for analyzing a platformless orientation system on a universal digital computer. 2 Figures, 3 references.

UDC 531.383

Resonance Methods of Monitoring Axial Unequal Stiffness of Gyromotor. V. Ye. Petrenko and A. I. Batov, p 54

Theoretical substantiation of methods of checking the axial unequal stiffness of the ball-bearing seats of a gyromotor that use the measurement of deviations of the natural frequencies of the gyromotor-vibration table system due to variation of orientation of the gyromotor axis in a gravity field is given. Measurement of the amplitude of the second harmonic of gyromotor oscillations with the gyromotor axis in the vertical and horizontal position is presented. Based on analysis of the errors, the advantages of the method that uses the amplitude of the second harmonic of the gyromotor oscillations with the gyromotor axis in the horizontal position is shown. 7 References.

UDC 531.383

Selection of Parameters of Elastic Damping Elements of Gyroscope. V. Ye. Petrenko and S. A. Zakharenko, p 59

The sequence of selecting the parameters of the flexible damping elements of a gyroscope for damping resonant oscillations of the gyromotor without reducing the vibration stability of the gyroscope is presented. The criteria

of optimization of values subject to selection are considered. Functions that permit one to determine the optimal values of the parameters to be selected for flexible damping elements, consisting of a metal spring and polymer interlayer, are found in dimensionless form. 4 References.

UDC 532.516:531.383

On Effect of Rotation of Body on Stability of Solid in Floated Suspension. Yu. V. Radysh, p 63

The equilibrium of a nonrotating spherical solid in a rotating spherical cavity of a body filled with an incompressible viscous liquid is studied. On the assumption of smallness of Re numbers, the perturbed motion of the solid in the cavity of the body is described by a system of linear integral equations of the Volterra type. The stability of the trivial solution of these equations is studied. Sufficient conditions are found for the stability of equilibrium upon arbitrary rotation of the body. The effect of special rotational modes on stability is studied. 4 References.

UDC 534.014

Comparison of Oscillations of Flexible Systems Exposed to Harmonic and Random Effects. I. I. Reznikov and L. M. Ryzhkov, p 69

The oscillations of flexible systems with distributed and concentrated parameters exposed to random and harmonic effects are studied. The reaction of the flexible system to harmonic and random effects is compared. 1 Reference.

UDC 629.1.053.11

Intercardinal Deviation of Controlled Gyrocompass With Different Types of Rolling. D. V. Reut, p 74

The errors of a controlled gyrocompass at different types of rolling are considered. Cases of the joint effect of different types of rolling on the instrument in which an additional systematic error appears in the readings are analyzed. 7 References.

UDC 531.768

On Systematic Error of Liquid Flywheel Switches Upon Positive Vibration of Base. Yu. N. Rudyk, V. S. Yevgenyev, and L. M. Shalda, p 79

The linear mathematical model of a liquid flywheel switch (ZhMP) under conditions of intensive vibrational perturbations in the absence of parametric resonance is studied. A formula is found for calculating the systematic error of a liquid flywheel switch. The resonance oscillations of the gas bubble of the liquid flywheel switch are studied in three main cases of combination of

the frequencies of natural vibrations of the liquid fly-wheel switch and vibration effects. Formulas are derived for determining the systematic error of a liquid flywheel switch for each of the considered cases of resonance oscillations. 2 Tables, 6 references.

UDC 531.768

Dynamic Characteristics of Pendulous Accelerometer With Flexible Suspension. V. M. Slyusar, A. V. Vyt-senko, and N. A. Gorbachev, p 84

The characteristics of the dynamics of a compensation pendulous accelerometer, determined by the specifics of its flexible suspension, are investigated. The calculated model of a mechanical system in which the practically feasible variation of the parameters of the flexible elements and the finite pliancy of the suspension in two additional directions are taken into account, is found. The effect of the resonance properties of the pendulum on the stability of the compensation accelerometer is estimated. 1 Figure, 3 references.

UDC 551.46.03

Method of Calculation of Parameters of Wire Rope, Exposed to Irregular Flow of Liquid. V. A. Yagodzin-skiy, p 88

A method is proposed for calculating the stress, angle of inclination, length and point coordinates of a wire rope exposed to the effects of an irregular liquid flow. The problem is solved in quasi-steady approximation by using dimensionless Poud table functions. 2 Figures, 2 references.

UDC 62-50

Asymptotic Estimation of State of Linear Dynamic System With Variable Parameters. S. M. Vavilov, p 90

It is suggested that the asymptotic identifier of state, which is constructed with "frozen" parameters of the system, be used to estimate the state of a linear dynamic system with variable parameters. The error of estimation determined by this identifier is found. The results are used in the problem of damping small oscillations of a horizontal gyrocompass with regard to information about the vector of relative velocity of the suspension point. 1 Table, 5 references.

UDC 531.36;531.31;531.391

Construction of Optimal Lyapunov Functions and Systems of Equations of Comparison for Study of Stability of Gyroscopic Systems. V. P. Deminenko, V. A. Rusin, and A. M. Semibolotnyy, p 95

A method is outlined for constructing the optimal Lyapunov functions by combining the connection of the first integrals of the equations of motion of gyroscopic

systems with construction of the majorizing function for the complete time-derivative of the Lyapunov function. The criterion of optimality is given in the form of a special index of the smallness of the difference equation between the input function and the majorizing function. Conditions are indicated for constructing a system of comparison equations, the upper solution of which is majorizing for the Lyapunov function in the entire range of phase space. 7 References.

UDC 537.3:629.7.05

On Construction of Methods of Converting Quasi-Coordinates to Coordinates of Orientation Vector. A. P. Panov, p 100

A new method of constructing the methods of conversion of quasi-coordinates (gyroscope readings) to coordinates of the orientation vector is considered. The possibilities of the method are shown on examples of constructing one-step methods of third and fourth orders of precision and of estimates of their errors. Ten third-order methods and 10 four-order methods are presented, including new methods having maximum small computing complexity. 1 Table, 5 references.

UDC 681.52

On Selection of Parameters and Structures of Controlled Systems From Criterion of Twofold Invariance. V. V. Udilov, p 105

The problem of analysis and synthesis of linear stationary dynamic systems, proceeding from the requirements of invariance to external perturbations and internal noise, is solved on the basis of the theoretical group approach. The consideration is given on the example of one of the classes of second-order systems with two inputs and one output. 1 Table, 2 references.

UDC 681.51

Homotopic Structures in Study of Invariance of Distributed Systems. A. S. Khokhlov, p 114

Postulations of the problem of strong and weak invariance for distributed systems are proposed in the paper by using the geometric language of description of differential equations with partial derivatives. The criteria of controllability and invariance are proved. 4 References.

UDC 531.01:513.83

On the Homotopic Theory of Adaptive Processes on Manifolds. Ye. S. Shcherbina, p 118

Problems of constructing the theory of adaptive processes on manifolds are considered. The geometric criterion of adaptability is shown. 5 References.

Vol 5, 1986

*81440686 Kiev MEKHANIKA GIROSKOPICHESKIKH
SISTEM in Russian Vol 5, 1986 (signed to press
21 Nov 84) pp 138-144*

[Abstracts of articles appearing in "Mechanics of Gyroscopic Systems," 1986]

[Text]

UDC 531.383

Precession Equations of Asymmetrical Fast-Rotating Body. O. F. Boychuk, pp 3-5

Equations of precession theory are found for a fast-rotating solid, the axis of rotation of which is not the axis of dynamic symmetry, on the assumption that the angular rate of natural rotation is considerably greater than the angular rate of rotation of the accompanying trihedron. 2 Figures, 2 references.

UDC 621.375

Calculation and Analysis of Static Error of Laser Gyroscope With Constant Displacement. Ye. A. Bondarenko, pp 6-9

Formulas are found for calculating the constant error component of a uniformly rotating laser gyroscope. It is established on the basis of analysis of the formulas that this error component is dependent on the angular rate of rotation of the gyroscope, on the time of accumulation of its output signal, and also on the parameters that characterize the zero drift, interaction of counter waves through reverse scattering and deviation of the data card value of the scale coefficient on its actual value. 3 References.

UDC 65.501:531.383

Identification of Parameters of Gyroscope in Automated Test Mode. A. V. Zbrutskiy, V. K. Cherniy, and G. M. Vinogradov, pp 10-13

An algorithm is proposed for identifying the parameters of a gyroscope in the automated test mode, based on regression analysis and least squares methods. The layout for conducting the experiment is constructed with regard to optimal planning methods. Experimental results are presented. 6 References.

UDC 537.311.32:532

On Parametric Resonance of Electrolytic Angle Converters. N. A. Ivanov, V. S. Yevgenev, Yu. N. Rudyk, and L. M. Shalda, pp 14-16

The mechanical model of an electrolytic angle converter (EPU), installed on a positive-vibrating base, is described. Using A. N. Andronov-M. A. Leontovich's diagram, the inertial mass characteristics of the air bubble of the electrolytic angle converter, which has a significant influence on the appearance of parametric resonance, are determined from the results of experimental studies. 1 Figure, 4 references.

UDC 531.383

On Decrease of Drift of Integrating Gyro With Irregular Rocking of Base. V. V. Karachun, pp 16-19

The functional composition is determined and the systematic component of the drift of an integrating gyro with two-channel automatic compensation of the effect of external noise with angular arbitrary oscillations is analyzed. 1 Reference.

UDC 531.385

Gradient-Frequency Control of Redundant Structures of One-Axis Force Gyroscopes. Yu. A. Karpachev, pp 20-28

A gradient frequency control algorithm, stable to systematic perturbations and one which minimizes the singular states of the gyro system, is synthesized for an arbitrary redundant gyro force system consisting of one-axis force gyroscopes (gyrodynes), rigidly bound to the housing of the body, with regard to limited angular precession rates. The relationship of the determinant and of the natural values of the gyro force Graham matrix to the geometric structure of the gyro system is revealed, which opens the paths for construction of rational structures and effective control of redundant gyro force systems. 4 References.

UDC 531.383

Synchronization of Autooscillations in Differential Vibration-Frequency Accelerometers. N. M. Lokot and V. M. Slyusar, pp 28-33

The synchronous operating modes of differential vibration frequency rod-type accelerometers are studied to work out design measures that permit one to reduce to a minimum the width of the frequency range of synchronization. The problem reduces to analysis of the interaction of two parametrically connected autooscillation contours with similar natural frequencies. 1 Figure, 4 references.

UDC 531.383

On Dynamic Model of Gyrocompass With Liquid Torsional Suspension. M.-A. Pavlovskiy, L. M. Ryzhkov, V. V. Avrutov, and V. F. Krishtal, pp 34-38

The dynamics of a single-rotor correctable gyrocompass with liquid torsional suspension is studied upon vibration of the base over a wide frequency range. The dynamic models of the instrument are determined at different excitation frequencies. 2 Figures, 3 references.

UDC 534.015:621.828

Characteristic Features of Describing Variations of Axial Stiffness of Rotary System. V. Ye. Petrenko, A. N. Belyakov, Ye. G. Levchuk, and A. I. Batov, pp 39-50

It is shown that approximate analytical expressions, found on the basis of expansion of H. Hertz' contact function into a Taylor series, permit one to describe the variation of axial stiffness with accuracy sufficient for practice. The given analytical formulas can be used to diagnose the state of ball-bearing seats with preliminary approach of the races. 5 Tables, 1 figure, 9 references.

UDC 534.015

Comparative Analysis of Two Dynamic Methods of Determination of Stiffness. V. Ye. Petrenko and S. V. Novikov, pp 50-57

It is shown by using two hypotheses of energy dissipation in a structure based on the proposed criteria of comparison of dynamic methods that the antiresonant method is preferable for minimizing the amplitude of cyclic deformation of the ball bearings of a gyromotor and of its variation, upon realization of which one can provide the steepness of the peak, similar to that of the resonance peak. Selection of the hypothesis of frequency-independent damping or of scattering according to Kelvin-Voight hypothesis has an insignificant effect on the results of analysis of antiresonant and resonant oscillation modes at the values of damping and ratio of masses, ordinarily encountered in gyroscopes. 3 Figures, 3 references.

UDC 629.7.054'847

Nonlinear Equations of Motion of Tuned Rotor Gyroscope in Astatic Coordinate System. V. P. Podchezertsev and B. L. Sklyar, pp 57-63

A system of equations of motion of the rotor of a tuned rotor gyroscope (DNG) in an astatic coordinate system is found on the basis of precise kinematic ratios of the gimbal suspension with regard to the response of the drive. The boundaries of applicability of the condition of dynamic tuning, derived for the linear model of a tuned rotor gyroscope, are determined. The errors of the gyroscope, caused by the geometric nonlinearities of the gimbal suspension and of the response of the drive, are calculated. 3 Figures, 6 references.

UDC 629.12.053.11

Interlocking of Azimuth and Horizontal Tracking Systems of Correctable Gyrocompass. D. V. Reut, pp 64-68

The effect of interlocking of the azimuth and horizontal tracking systems of a correctable gyrocompass, caused by moments of dry frictional forces, on its dynamics is studied. The qualitatively different effect of the time

constant of the horizon display on the amplitude of autooscillations is shown as a function of the point of currents of the friction in the system. 7 References.

UDC 629.197.31

On Displaying of Gyro Platform on Fixed Base. A. A. Bezbogov, pp 68-70

The problem of the initial display of gyro platforms (GP) of inertial navigation systems, mounted on a movable base, is considered. The possibility of display is shown when using additional information about the mutual motion of the driven and driving gyro platforms. 2 References.

UDC 534

Nonlinear Oscillations of Linear Acceleration Integrating Gyro on Movable Base. V. I. Gulyayev, P. P. Lizunov, and V. A. Saushev, pp 71-75

The effect of variation of the moment of the stabilizing motor and of the frictional coefficients in the bearings of the gimbal axes on the angles of rotation of the outer race and of the gyrochamber of a linear acceleration integrating gyro with different types of vibration of the base is studied. An algorithm, based on the method of continuation of the solution with respect to the parameter, is used to construct the periodic solutions of the equations of motion. 1 Figure, 4 references.

UDC 534.1:624.07

On Structure of Acoustic Field Inside Cylindrical Shell. V. S. Didkovskiy, O. N. Ivanova, A. V. Kuzmenko, and G. N. Pelipenko, pp 75-78

An approach is suggested that permits one to describe, along with acoustic pressure, the oscillations of a thin cylindrical shell and an arbitrary angle of incidence of the acoustic wave. 1 Figure, 2 references.

UDC 621.002.5

Calculation of Stiffness of Gimbal Elements. S. A. Zakharenko and A. Ye. Ponomarenko, pp 78-83

A method is developed for calculating the stiffness of gimbal elements (gimbal disks) of arbitrary cross-section. The finite difference method and potential energy method are used. Analytical functions are found for calculating disks with rectangular and trapezoidal shape of cross-section. 2 Figures, 6 references.

UDC 531.383

On Stabilization of Mechanical System of Gyroscopic Forces. K. R. Kovalenko, pp 83-86

Proof of Kelvin's theorem, distinct from ordinary theorems, on stabilization of the motion of mechanical systems by gyroscopic forces as a result of suggesting the stability of solutions of canonical systems in the indefinite case is outlined. 2 References.

UDC 531.383

On Small Oscillations of Rapidly Twisted Solid in Unequal Stiffness Contactless Suspension. Yu. G. Martynenko and A. V. Medvedev, pp 86-91

The motion of a solid with arbitrary ellipsoid of inertia, located in some force field, is considered. The evolutionary equations of angular motion are constructed by using the method of averaging and the conditions of asymptotic stability of nutational oscillations upon rotation of a body about the axes of the largest and smallest moments of inertia are derived. The range of asymptotic stability of nutational oscillations in a plane of parameters that characterize the properties of the suspension is constructed for specific parameters of the body and for the transfer function of the suspension. 2 References.

UDC 532.516:531.383

Determination of Forms of Flow of Liquid in Floated Suspension. Yu. V. Radysh, A. S. Kireyev, and O. P. Marosin, pp 91-95 One method of selecting the coordinate functions used in simulation of the dynamics of an incompressible Newtonian liquid finite-dimensional approximation is suggested. The boundary value problems are formulated with respect to the desired functions and a procedure is described for solving them by the finite element method in a range typical for floated gyroscopes. 1 Figure, 6 references.

UDC 532.516:531.383

Taking Into Account Symmetries of Liquids and Solids in Structure of Equations of Dynamics. Yu. V. Radysh and A. I. Yurokin, pp 96-100

The motion of a system of liquids and solid in finite-dimensional approximation is described by differential equations of dynamics in quasi-coordinates. The structure of the equations of dynamics of implicit type is studied on a specific example. The general properties of the coefficients of the equations are indicated. The special properties of coefficients generated by the symmetries of the mechanical system are established according to the proposed method. The method is easily algorithmized and is easily realized on the computer. 4 References.

UDC 534.014

On Oscillations of Systems With Distributed Parameters Upon Kinematic Random Excitation. L. M. Ryzhkov, pp 101-104

Expressions are found on the example of vibrations of a plate for absolute accelerations of the oscillations of systems with distributed parameters during kinematic random excitation. It is shown that these accelerations upon vibration of the base with acceleration of the white noise type approach infinity. 2 References.

UDC 681.5

Minimax Approach to Parametric Identification of Dynamic Systems. A. V. Zbrutskiy and T. V. Prokopchuk, pp 104-108

An algorithm is worked out for identification of a dynamic system based on the minimax approach and a method is proposed that realizes the given algorithm as the most effective. 1 Table, 6 references.

UDC 531.385

Different-Module Control of Minimal Excess Coplanar Structure of Gyrodynes With Orthogonally Oriented Suspension Axes of Gyro Assemblies. Yu. A. Karpachev and M. A. Pavlovskiy, pp 108-118

A new principle of programmed control of a gyro system, the one-axis force gyroscopes of which are distributed in two orthogonally oriented groups in each of which the suspension axes of the gyro assemblies are parallel to each other, is considered. Control is based on expansion of the vector of the kinetic moment into two equal-module vectors. It is shown that equal-module control minimizes the set of singular states of the gyro system and results in simpler and inertialless algorithms for calculation of the programmed angular rates of precession of the gyrodynes. 6 Figures, 4 references.

UDC 531.01:531.383

Algebraic Structure Observed in Quantum Gyroscopy. Ye. S. Shcherbina, pp 119-127

Different algebraic structures that occur in quantum gyroscopy are considered. The properties of races to be observed for quantum and classical dynamic systems are presented. The properties of Li and Jordan algebras, which are typical for gyroscopic systems designed on quantum gyroscopes, are indicated. 1 Figure, 8 references.

UDC 621.01

Programming of Motions of Manipulator Gripper With Excess Degree of Mobility. V. A. Yagodzinskiy and Ye. V. Nedosekov, pp 128-131

A linearized algorithm for solving the inverse problem of kinematics for a seven-link manipulator, one of the degrees of mobility of which is selected on the basis of the structural limitations of the mutual angular position of the

other pair of links, is developed. Program module designed for real-time calculation of the programmed motion of the gripper are indicated. 1 Figure, 2 references.

UDC 519.3

Decomposition of Nonlinear Controlled Systems With Group Symmetry. G. N. Yakovenko, pp 131-137

The concept of the group of symmetry, permitted by a system with control, is introduced. The results are presented that permit one, on the basis of the group of symmetry of transition to another variable, to achieve decomposition in the system. 4 References.

Vol 6, 1987
81440686 Kiev MEKHANIKA GIROSKOPICHESKIKH SISTEM in Russian Vol 6, 1987 (signed to press 21 Nov 84) pp 134-142

[Abstracts of articles appearing in "Mechanics of Gyroscopic Systems," 1987]

[Text]

UDC 531.383

Study of Cross Connections in Gimbal Suspension of Tuned Rotor Gyroscope. I. V. Balabanov, pp 3-6

A method of calculating the flexible characteristics of tuned rotor gyroscope suspension of complicated three-dimensional design is shown. The possibility of eliminating the harmful cross connections in the flexible axes by assuring the symmetry of their design is considered. The effect of practically feasible errors of manufacture and assembly of the suspension and is elastic characteristics are studied. 1 Figure, 2 references.

UDC 62-752.4:621.375.826

Calculation and Analysis of Static Error of Laser Gyroscope With Sign-Variable Displacement. Ye. A. Bondarenko, pp 6-9

Formulas are found for calculating the constant error component of a uniformly rotating laser gyroscope with displacement having the form of sign-variable square-wave pulses. It was established on the basis of analyzing the formulas that this error component is dependent on the angular rotational velocity of the gyroscope, on the time of accumulation of its output signal and on switching the magnetic field of the difference frequency element. It is also dependent on the parameters that characterize zero drift, interaction of counter waves through reverse scattering, deviation of the data card value of the scale coefficient from its actual value and the difference in the length of different-pole displacement pulses. 5 References.

UDC 531.383

Quadrature Drift of Tuned Rotor Gyroscopes. A. V. Zbrutskiy, N. P. Shevchuk, and V. M. Vinogradov, pp 10-18

The reasons for the occurrence of quadrature drift of tuned rotor gyroscopes, caused by elastic deformations of the suspension, are studied. The types of symmetry of the gimbal suspension of single- and two-race gyroscopes in which there is no drift are established. Analytical expressions are found for estimating the effect of technically feasible errors of manufacture on quadrature drift. 1 Figure, 5 references.

UDC 531.383

Effect of Errors in Manufacture of Flexible Annular Resonator on Accuracy of Solid Wave Gyroscope. A. V. Zbrutskiy, S. A. Sarapulov, and S. P. Kisilenko, pp 18-23

Equations of motion of a flexible annular resonator on a rotary base are found with regard to the errors of manufacturing it. The effect of these errors on the dynamics of the resonator and on the accuracy of a solid wave gyroscope is considered. 1 Table, 3 references.

UDC 531.383

Generalized Form of Representation of Systematic Error of Ground Gyrocompass Caused by Vibration. Yu. F. Lazarev and P. S. Mironenko, pp 23-27

A generalized mathematical model of the constant error component of a gyrocompass, installed on a vibrating base, is presented. This model is suitable for study of the different types of single-rotor gyrocompasses. The model is distinguished by compactness and clearness of the physical idea and is adaptable for comparative analysis of different layouts of gyrocompasses by numerical modeling on the computer. 2 Figures.

UDC 531.383

Interaction of Auto-Oscillations in Differential Vibration-Frequency Accelerometers. N. M. Lokot, pp 27-30

The interaction of the auto-oscillations of resonators in differential rod or string vibration-frequency accelerometers at different ratios of natural frequencies is studied. The effect of nonlinear phenomena in the converter on its characteristics is considered. 2 References.

UDC 531.383

Dynamics of Single-Rotor Correctable Gyrocompass With Angular Vibration of Base. M. A. Pavlovskiy, M. V. Chichinadze, and V. F. Krishtal, pp 30-35

A mathematical model is developed that describes the behavior of a gyrocompass upon angular vibration of the base. The error of the instrument is studied with regard to the dynamics of tracking systems. Analysis showed the existence of resonance frequencies, determined by the parameters of the stabilization circuits. 4 References.

UDC 531.383

Optimization of Parameters of Dynamic Damper of Nutational Oscillations of Gyroscope. V. Ye. Petrenko, S. A. Zakharenko, and A. Ye. Ponomarenko, pp 35-37

Analytical functions are found for calculating the optimal parameters of the dynamic damper of the nutational oscillations of a gyroscope. 4 References.

UDC 534.015:621.828

Diagnostics of Radial Thrust Ball Bearing as Dependence of Its Axial Stiffness on Practically Feasible Errors. V. Ye. Petrenko, Ye. G. Levchuk, and A. V. Tsukanov, pp 37-44

A method of test diagnosis of rotors that utilize the functional relationships between the harmonics of variation of the axial stiffness and defects of radial thrust ball bearings with axial tension, which ensures the full contact mode, is considered. The requirements are formulated on selecting the parameters of installation to check the stiffness of the ball bearings. 1 Table, 1 figure, 3 references.

UDC 531.768

On Effect of Thermodynamic Processes on Static Characteristic of Electrolytic Angle Converters. Yu. N. Rudyk, A. V. Salenko, V. S. Yevgenyev, and V. M. Kostyrev, pp 44-48

The effect of thermodynamic and electric processes that occur in electrolytic angle converters (EPU) on the type of static angle-current characteristic is considered. It is noted that heating the electrolytic angle converter affects the restoring moment, the time of the transient process and the static error, and also reduces the steepness of the static characteristic. It indicates the existence of ponderomotive forces, by which one explains the existence of a zone of insensitivity in the static characteristic of an electrolytic angle converter. The phenomenon of effervescence of the electrolyte and formation of bubbles in the electrolytic angle converter is considered. Recommendations are outlined to improve the stability of the characteristic of the electrolytic angle converter and to prevent boiling of the electrolyte. 3 Figures, 3 references.

UDC 531.768

Design of Digital Two-Component Compensation Angular Rate Meter. V. M. Slyusar and V. V. Tsisarzh, pp 48-51

The problem of designing a digital compensation angular rate meter with desired arrangement of the roots of a closed system in the w plane is considered. 1 Figure, 3 references.

UDC 531.768

On Selection of Parameters of Digital Compensation Linear Acceleration Meter. V. M. Slyusar, V. V. Tsisarzh, and Ye. V. Nedosekov, pp 51-54

Relations that permit one to design the parameters of both digital and analog filters are found which provide the required stability margin of a compensation linear acceleration meter at minimum implication factor of the high-frequency noise component at the input of the filters. 1 Figure, 1 reference.

UDC 534.013

Resonance Interaction of Forced and Self-Excited Oscillations in Rotor System. Z. T. Cherneva-Popova, pp 54-59

The interaction of forced and self-excited oscillations in a rotor system, consisting of two disks connected by a flexible shaft, in the resonance region is considered. Self-excitation of the vibrations is determined by the influence of dry frictional forces. A system of differential equations of motion for steady modes is solved by the averaging method. The effect of the physical parameters of the system on formation of the vibration characteristics in different cases of excitation is analyzed. 3 Figures, 4 references.

UDC 531.383

Dynamics of Two-Mode Directional Gyroscope With Nonlinear Characteristic of Flexibility of Gimbal Suspension Axes. I. K. Shubin, pp 59-66

The dynamics of a two-mode directional floated gyroscope with stiff gimbal suspension axes on a vibrating base is studied. Three types of flexibility characteristics of the axes are considered: linear, nonlinear of cubic parabola type, and nonlinear with finite stiffness limiter. The laws of stable oscillations and the amplitude frequency characteristic of the gyroscope are determined. Formulas are presented for the constant components of the azimuth errors of the gyroscope in the gyrocompass mode. 2 Figures, 5 references.

UDC 621.01

Planning of Specific Positions of Gripper With Regard to Restrictions of Mobility of Manipulator Sections. L. Yu. Akinfiyeva and V. A. Yagodzinskiy, pp 66-69

An algorithm for planning the specific displacement of a gripper without preservation of orientation is developed. The algorithm permits one to assure the mobility of manipulator sections having structural limits. 1 Figure, 3 references.

UDC 531.01

Optimal Damping of Daily Fluctuations of Inertial Navigation Systems. O. F. Boychuk, pp 70-74

The general layout of optimal control of linear objects with a degenerate matrix of control quality is presented. Examples of precise solution of the problem of optimal damping of daily fluctuations in inertial navigation systems in the presence of one and two measurements with white noise in the system and in the measurements are given. The problematical nature of damping daily fluctuations by one information source is shown. 4 References.

UDC 007.62

Compensation of Dynamic Effects on Drive of Manipulation Robot During Control of Its Motion. V. S. Yevgenyev and S. G. Bublik, pp 75-77

A method is outlined for computer calculation of the reduced moments of inertia of the actuating member of a manipulator, based on linearization of coordinate transformation matrices. It is shown that linearization permits one to determine the increments of the moments of inertia and gravity of the manipulator sections on each cycle of the calculations and to provide controlled motion with regard to dynamic loads in real time. 1 Figure, 2 references.

UDC 531.3:629.7.05

Kinematic Synthesis of Control of Terminal Reorientation of Solid in Space. Yu. A. Karpachev, pp 78-85

A suboptimal-speed inertialless algorithm for electric flywheel control of the terminal reorientation of a spacecraft with respect to a program basis of orientation, rotating steadily in inertial space is developed. It is shown that the rotational axes of the flywheels should be uniformly distributed and oriented in the directions of the lateral ribs of a regular multisided pyramid, fixed in the axes of the spacecraft, in optimal arbitrary-redundant electric flywheel actuating members. 7 References.

UDC 532.516.531.383

On Stability of Solid in Floated Suspension. Yu. V. Radish and M. A. Pavlovskiy, pp 94-98

The stability of the position of equilibrium of the center of an internal sphere during joint rotation of the spheres about central axes is studied with respect to a mechanical

system, consisting of a spherical solid and incompressible viscous liquid, which are enclosed in a spherical cavity of the supporting solid. The range of stability in the space of parameters of the mechanical system is determined. The limitation of the methods of hydrodynamic theory of lubrication upon study of the stability of solids in floated suspensions is shown. 5 References.

UDC 532.516:531.383

Moment Formation in Floated Suspension of Solid Upon Jet Flow of Liquid. Yu. V. Radish, pp 99-104

A mechanical system, consisting of a solid and incompressible viscous liquid, which are enclosed in the spherical cavity of the supporting body (housing), is considered. The solid is suspended at a point fixed with respect to the supporting body. The liquid fills a multisection cavity between the solids. The mechanism of occurrence of a hydrodynamic moment acting on the solid is revealed with jet nature of flow of the liquid due to the effect of internal forces. 2 References.

UDC 534.014

Vibrations of Systems With Imperfect Elasticity of Material During Random Excitations. I. I. Reznikov, L. M. Ryzhkov, and S. N. Osipchuk, pp 105-108

The vibrations with systems with imperfect elasticity of the material during steady random excitation are studied. Comparative analysis of the analytical solution of the nonlinear equation to the results of computer solution of the equation, which confirms the rather precise agreement of them, is given. The substantiation of the adopted assumption that the vibrations can be considered in the form of a normal steady random process in real systems of this type upon steady normal effects is shown. 2 Tables, 7 references.

UDC 534.014-531.383

Study of the Perturbing Moments Acting on Structural Elements of Instruments. L. M. Ryzhkov, pp 109-113

The characteristic features of finding the systematic components of the perturbing moments upon random effects related to the type of mutual spectral densities are considered. The integrated form of mutual spectral densities is proposed. The use of the integrated form of mutual spectral density for determination of the mean value of the perturbing moment is shown on the example of the elastic unbalance moment. 3 References.

UDC 519.3:62-50

Phase Structure of Partial Aggregation of Dynamic System. T. G. Smirnova, pp 114-118

A dynamic system that permits partial aggregation, i.e., a system, which may result in a form that the right sides of some equations will be dependent on a smaller number of equations than in the initial system by use of degenerate replacement of variables is considered. A case is investigated when the dynamic system permits some set of M methods of partial aggregation. It is shown that set M can be divided into classes of equivalence and the set of classes of equivalence is the structure. 3 References.

UDC 532.516

On Determination of Hydrodynamic Fields in Layer of Liquid Flowing Along Surface of Horizontal Rotating Disk. T. V. Sirzhik and L. M. Shalda, pp 119-122

The problem of flow of an incompressible viscous liquid, delivered under pressure to a horizontal rotating disk, is solved in approximation of the boundary layer. Functions are found that determine the thickness and rate of film flow as functions of distance to the rotational axis and of the number of parameters of the process. The results of calculation are in agreement with experiment and find application in design of centrifugal devices. 3 Figures, 1 reference.

UDC 620.178

On Study of Relay-Sliding Auto-Oscillations of Systems With Dry Friction. S. A. Chernikov, pp 123-127

An approximate method of investigating relay-sliding periodic modes in nonlinear systems with dry friction is developed. The method, based on harmonic linearization of the nonlinear characteristic and on consideration of higher harmonics in the expansion, permits one to take into account the "jumps" of derivatives, caused by nonlinearities. An example of calculating a nonlinear system—a uniaxial gyro stabilizer with dry friction in the suspension axes—is given. 5 Figures, 4 references.

UDC 621.372.8

Fiber-Optic Elements of Specialized Calculator To Compress, Contour, and Filter Image Signal

18610437 Novosibirsk AVTOMETRIYA in Russian No 1 Jan-Feb 89 pp 95-97

[Article by A. V. Bochkarev, A. V. Loginov, M. Ya. Mesh, I. M. Ovchinnikov, A. L. Shlifer, and G. A. Yudin, Novosibirsk-Tashkent]

[Text] An algorithm, schematic, and the characteristics of a fiber-optic specialized calculator for determining the displacement of a forward-moving object were examined previously.[1] This device can operate at clock frequencies up to 40 MHz, which is significantly faster than is the information input provided by existing high-speed image receivers (whose rate is 10 MHz or less). This difference between the speed of the fiber-optic specialized calculator and the speed at which information is input into it makes it possible to use the specified calculator to track several objects (in the case where several image receivers are sequentially polled) in real-time or to organize additional image-processing operations. In these cases, time compression of the image-scanning signal may be used to match the relatively slow image receiver and the high-speed fiber-optic specialized calculator. This operation may be implemented by using the component base used in the fiber-optic specialized calculator, i.e., it may be implemented on the basis of a fiber-optic annular structure analogous to the one examined previously.[1]

We will introduce the key parameters of the line-by-line image-scanning signal and the fiber-optic annular structure. Let the frame-scanning signal contain N pulses with a relative duration (Q) equal to or greater than 2N and with a pulse spacing of τ. Let the time of the cycle in which the signal references the fiber-optic annular structure equal T. When

$$T = (N - 1)\tau/N, (1)$$

the i-th pulse (i = 1 to [N - 1]) passing along the fiber-optic annular structure appears at the output, arriving in τ/N before the (i + 1)-th pulse passing through, i.e., the pulse repetition rate becomes equal to τ - T. The N-fold time compression of the pulse sequence is thus achieved.

The signal's fiber-optic annular structure cycle time is related to the length L of the fiber-optic light pipe by the relationship

$$T = (L_n/c) + t_{el}, (2)$$

where n is the refractive index of the light pipe's core, c is the speed of light in a vacuum, and t_{el} is the delay in the electrical circuits of the fiber-optic annular structure. Hence, achieving the N-fold compression of a sequence of N pulses requires a light pipe with the length

$$L = [(N - 1)c\tau/Nn] - [t_{el}(c/n)], (3)$$

which, for example, when N is approximately 10^3, t_{el} is about 10^{-8} and τ is about 10^{-5}, amounts to approximately $2 \cdot 10^3$ m, i.e., scanning of a 32x32-element frame with a clock rate of about 100 kHz can rather easily be compressed 1,000-fold by using a fiber-optic annular structure. It is thereby rather easy to match a photodetector matrix operating at a relatively low frequency (about 100 kHz) with the fiber-optic specialized calculator.

It should be noted that the compression operation is completed with the arrival of the N-th pulse, i.e., it does not result in any time loss when the signal is processed.

In our experiments we used a fiber-optic specialized calculator with a period T of about 750 ns (L, approximately 150 m). Depending on the clock rate selected at the input within the range from 1.3 to 8.9 MHz, it was possible to compress an input sequence in which the number of pulses (N) was between 3 and 20 pulses 3- to 20-fold, respectively. Figure 1 [not reproduced] presents an oscillogram of the compression process when N = 4 (sequence 1011) with a pulse repetition rate at the input (τ) of approximately 920 ns. At the moment when the last pulse arrives at the input of the fiber-optic specialized calculator, a sequence with a pulse repetition rate of about $0.2\mu s$ appears at its output.

The fiber-optic specialized calculator may thus be used as a pulse sequence compressor.

The functional capabilities of the fiber-optic specialized calculator may be expanded by implementing other image processing functions, for example, identifying its contour or filtering it.

When identifying contour elements it is necessary to shift the image one element along the vertical and horizontal and determine the elements of the original and shifted images that do not coincide. The time registration of the elements $x_{i,j}$ and $x_{i+1,j+1}$ is thus implemented, and the modulus of the difference in the values of these elements is determined. For the case of a binary image this corresponds to finding the gradient of the function of the distribution of the brightness in a diagonal direction.[2]

Thus, in the example examined, the contour is determined in accordance with the expression

$$\text{absolute value } x_{i,j} - x_{i+1, j+1} \text{ absolute value} = 1. (4)$$

We will note that the gradient of the brightness function in the vertical and horizontal directions may be found analogously.
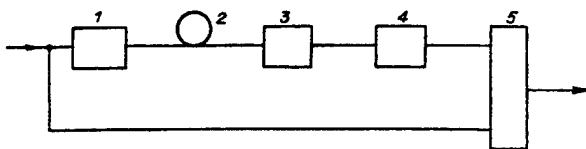
Figure 2

Figure 2 is a schematic of the contour identification device. The radiation source (1), fiber light pipe (2), photodetector (3), and shaper (4) (to restore the fronts and level of the signal received) represent a fiber-optic delay line. The signal delay t in this line

$$t = (M +/- 1)\tau \ (5)$$

(M being the number of elements in a line) corresponds to the shift of the original image one element to the right (left) downward. The "shifted" image is compared with the original image in the image-scanning time in an "exclusive OR" element (5), at the output of which the signal corresponds to the scanning of the image contour. When τ is approximately 33 ns and when the image is 32x32 elements in size, this operation is performed within about 1 μs and requires about 200 m of fiber light pipe.

Figure 3 presents oscillograms of the scanning of a 4x4-s element that has been shifted (M + 1) elements with a 3x3 object in it (top) and the contour corresponding to this object (bottom) when τ is about 0.17 μs and L = 200 m. It is evident that the pulse sequence corresponding to the scanning of the contour occurs at a rate that is matched with the arrival of the shifted image signal.

We will note that the device for identifying the image contour may be included as a component of the fiber-optic specialized calculator described above. This does not require any structural changes in the latter.
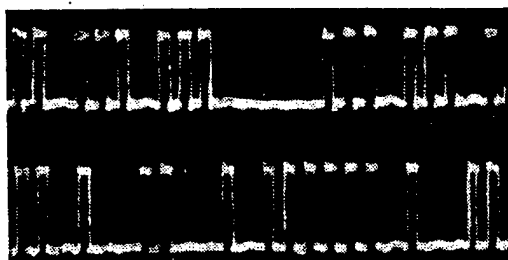

Figure 3

Besides the contour identification device examined, the fiber-optic specialized calculator may be used as a basis for creating image filtration devices. The "local averaging of each element in an image with respect to its adjacent elements"[2] may, for example, lie at the foundation of the operation of such filters, or they may use recurrent digital filtration.[3] In any case, the fiber-optic specialized calculator makes it possible to obtain a scan of etalon frames and thereby implement the time registration of the signals of some image elements or others with their subsequent summing and comparison with a specified threshold. Computer calculations have shown that using a filter based on the averaging of each element with respect to eight adjacent elements[2] as a component of a fiber-optic specialized calculator increases its noise immunity significantly. For example, with objects 16x16 elements in size and noise levels in the frame of 20 and 30 percent, the probability of an error in determining the shift amounts to 0 and 5 percent, respectively (without any preliminary filtration of the image, 10 and 20 percent[1]).

We have experimentally tested the elements of such a filter corresponding to filtration along the vertical, horizontal, or diagonal for an object 2x3 in size in a frame of 4x4 elements. They cleaned the noise fragments from the image. A set of such devices makes it possible to optimize the filtration process depending on the dimensions and shape of the image in the frame.

Thus, using fiber-optic delay lines and active annular structures significantly expands the functional capabilities of fiber-optic specialized calculators.

Bibliography

1. Loginov, A. V., Mesh, M. Ya., Ovchinnikov, I. M., et al., "Fiber-Optic Specialized Calculator for Determining Displacement of Forward-Moving Object, AVTOMETRIYA, No 1, 1989.

2. Rozenfeld, A., "Image Recognition," TIIER, Vol 69, No 5, 1981.

3. Sarnadskiy, V. N., "Using Recurrent Digital Filter in Processing Holographic Images," in "Golograficheskiye izmeritelnyye sistemy" [Holographic Measuring Systems], ed. by A. G. Kozachok, Novosibirsk, NETI, 1980.

UDC 551.515.3:621.039.5

Tornado Zones in the USSR and Siting of Nuclear Power Plants

[Article by F. F. Bryukhan, M. Ye. Lyakhov and V. N. Pogrebnayk, VGNIPKII "Atomenergoproyekt" and Institute of Geography of the USSR, Academy of Sciences]

[Text] Abstract: The principal tornado zones in the European Territory of the USSR are identified based on historical data and observations over the last few years, the meteorological conditions under which tornadoes arise are analyzed, and a method for calculating tornado probabilities is proposed. These data must be taken into account in order to build objects whose destruction is especially dangerous.

Tornadoes are the most dangerous meteorological phenomena capable of destroying buildings and structures [3,4]. The destructive power of tornadoes is caused not only by the enormous (up to 150-220 m/sec, and according to estimates by P. Dergarabedyan and F. Fendel up to 300 m/sec) wind velocities and power of the wind impact, but also by the sharp drops of the atmospheric pressure between the periphery and center of the vortex. The pressure gradient in the region of a tornado is estimated to be 10 hPa/100m[8].

As a tornado passes the air pressure can drop rapidly by 100-200 hPa. The large differences in the air pressure arising in the process outside and inside closed buildings often causes the buildings to "explode." The walls of houses in such cases fall away from the framework, and objects inside the building, sometimes including people also, are sucked out of the rooms. The rising air currents in a tornado reach velocities of 70-80 m/sec.

In the USSR tornadoes from several tens of meters to 1 km in diameter have been observed. The translational velocity is approximately 40-60 km/h. the maximum length of a tornado path is 100-120 km.

In the USSR the climatology of tornadoes had not been studied until recently. It was thought that not enough information existed about tornadoes to make such a study. A great deal of information about tornadoes in different regions of the country has been accumulated over the last hundred years, especially for the European Territory of the USSR (ETU), enabling the study of the spatial distribution of tornadoes and determination of tornado probabilities in any given region. The first climatological works on tornadoes were published only in the last two years[2,5]. In [2] information about tornadoes based on both modern observations and historical information dating back to the thirteenth century is

employed. Reference [5] gives a list of tornadoes recorded over the period 1844-1986, which turned out to be incomplete and, for use in this work, was supplemented by data obtained by M. Ye. Lyakhov.

Despite their discreteness in time and space tornadoes can occur in clusters and they are found to be correlated with definite regions and zones. For example, in the twentieth century a large number of tornadoes in the Lithuania-Bellorussia region was observed in the periods 1950-1953, 1967-1969, and 1979-1983.

On the territory of the USSR tornadoes can be theoretically expected to appear, with greater or lesser probability, anywhere with the exception of mountain ridges and the Arctic. They have not infrequently been observed on the territory of the ETU from the shore of the Black Sea to the Solovetskiye Ostrova, from the western border to the Ural chain, and from the deserts and semideserts of Central Asia to the lower parts of the Ob River. There are data indicating that tornadoes also occur in other regions of Siberia.

Occurrences of tornadoes on the ETU are plotted on the map in Fig. 1. The envelope of tornado trajectories delineates a zone with high tornado density. There are four such zones: A—Lithuania, Bellorussia, and Pravoberezhnaya Ukraina; B—near Moscow, the Klyazmy-Meshcher Basin, Voronezh, Western Donbass—the lower parts of the Dnepr River—Northern Crimea; C—the Crimean coastline, the Sea of Azov, and Krasnodar kray; and, D—Sredney Kama and Udmurtiya Basin.

Analysis, over a period of many years, of the synoptic-aerological conditions under which tornadoes appear in the ETU has shown that the tornado synoptic situation and meteorological conditions are analogous in all cases. They develop under the conditions of meridional circulation of the atmosphere, when the frontal zones along which tornado clouds form assume a position close to the meridional position. In the process rapid flow of cold air masses from the Arctic into the southern regions and flow of warm tropical air far up to the north, characterized by strong vertical instability, occur.

The climatic tornado zones A and B, identified within the ETU (Fig. 1), correspond precisely to this position of the frontal zones. At the same time tornado occurrences are not distributed uniformly in these zones, but rather in sections. Three sections can be separated in each zone: 1) northern, predominantly forested with significant swampiness (A-F, B-F); 2) forest steppe (A-FS, B-FS); and, 3) southern steppe (A-S, B-S). Tornadoes occur more frequently in the first and third sections than in the second section. The less frequent occurrence of tornadoes from south to north is associated with the transformation of tropical air as it moves and partial loss of vertical instability. As air flows over a wetter underlying surface its moisture content increases, as a result of which it becomes more unstable owing to moisture liability and intensification of convection. This intensifies the development of thunderclouds
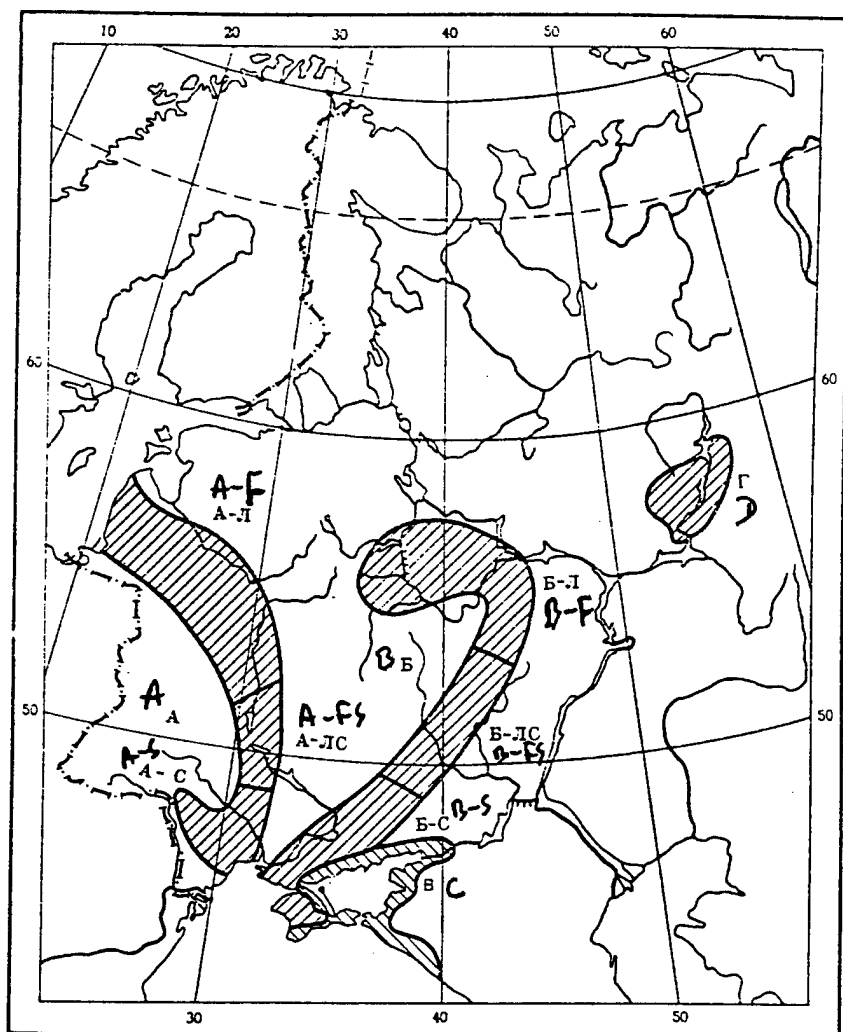
Figure 1. Tornado Zones in the European Territory of the USSR. The Characteristics Are Given in the Text.

and the appearance of vortices in them with both horizontal and vertical rotational axes. Apparently, for this reason tornadoes are often observed in the forested Vyatsko-Kama and Ural regions and are almost unknown in the Trans-Volga steppes.

Water surface temperature plays a large role in the appearance of tornadoes on the coast of the Black Sea. It is noted in the literature, including by A. I. Snitkovskiy in [5], that in order for tornadoes to form the water temperature in the Black Sea must not be lower than 24 degrees C. It should be noted, however, that tornadoes arise most often on the northern Caucasian coast and not on the southern coast, where the water temperature is higher. It is believed that it is not the water temperature itself that is most important, but rather the difference between the water and air temperatures, on which the vertical temperature gradients determining the instability of air masses depend. This question, no doubt, requires further study.

Thus the ETU contains distinct tornado zones; in adjacent regions tornadoes have been observed only rarely or not at all. However the occurrence of tornadoes within the tornado zones is still a quite rare event. For this reason the possibility of the occurrence of tornadoes and the burdens and disturbances associated with them must be taken into account only when designing objects that are part of the national economy and must meet special reliability requirements, in particular, in the design of nuclear power plants (NPP). To take into account the combinations of loads and disturbances from a probable tornado in designing buildings and structures at an NPP it is necessary to have statistically reliable estimates of the expected meteorological characteristics of the tornado. Modern safety requirements for NP make it necessary to take into account the theoretical loads from tornadoes even with very low yearly tornado-occurrence probabilities.

Because the climatology of tornadoes has not been adequately studied and because tornadoes do not occur often in the USSR the theoretical loads from tornadoes on buildings and structures at an NPP are still determined based on estimates made by experts. Under existing siting and construction regulations for NPP it is necessary to have a standard meteorological basis for calculating the characteristics of tornadoes in any region of the country. We propose the following probabilistic estimate of the expected class and characteristics of a probable tornado.

Consider a region with area A in which tornadoes have been recorded over a period of T years. The yearly probability for a tornado to pass through any point in a region with uniform climatic conditions for formation of tornadoes is defined as follows:

$$Ps = S/AT \quad (1)$$

where S is the total area of the tornado zone in the region under study over the observational period.

The characteristics of observed tornadoes can be measured only in rare cases, and most of the data on the passage of tornadoes are of a qualitative character. This makes it much more difficult to perform a climatological analysis of existing information on tornadoes. The Fujita-Pearson intensity scale assigns some approximate quantitative characteristics to tornadoes.[7, 9, 10] Based on this scale the intensity classes (integers from 0 to 5 inclusively) are determined based on qualitative descriptions. According to [9, 10], the characteristic values of the maximum rotational velocity of the wall of a tornado V_k and the length L_k and width W_k of the zone through which a tornado of class passes are determined with the help of the following empirical relations:

$$V_k = 6.3 \, (K + 2.5)^{1.5} \text{ m/sec}$$

$$L_k = 1.609 \cdot 10^{0.5(k-0.5)} \text{km} \quad (2)$$

$$W_k = 1.609 \cdot 10^{0.5(k-4.5)} \text{ km} \quad (0 \text{ less than or equal to } k \text{ less than or equal to } 5)$$

An analogous expression can be written down, following [10], for the translational velocity of a tornado:

$$U_k = \tfrac{1}{4} \, V_k = 1.575 \, (k + 2.5)^{1.5} \text{ m/sec} \quad (3)$$

In the Fujita-Pearson model the velocities v_k and u_k are determined solely by the intensity class. This is obviously also true for loads generated by a tornado. For this reason, we shall study not the statistics of the velocities or loads, but rather the statistics of the intensity classes.

The yearly probability for the occurrence of a tornado with class higher than k at a fixed point of a region is

$$P = P_s[1 - F(k)] \quad (4)$$

where F(k) is the probability that the class does not exceed k for tornadoes recorded in the given region. We denote by n_k the number of tornadoes of class k. In determining the total area over which tornadoes pass we shall keep in mind the fact that the actual number of weak tornadoes is greater than the observed number. We shall adopt the following dependence of the ratio of the number of actual tornadoes to the number of recorded tornadoes on the intensity class:

$$\alpha(k) \text{ coequals } \alpha_o \text{ for k less than or equal to 1 and 1 for k is greater than 1} \quad (5)$$

According to [5], the quantity α_O for regions with a low population density can vary from 2 to 4. Thus the total tornado-passage area can be written as

$$S = \sum_{k=0} n_k \alpha \, (k) \, L_k W_k \quad (6)$$

where 1 is the lowest observed class.

The empirical probability of a tornado of class k at a fixed point is proportional to the tornado-passage area:

$$(k) = \alpha(k) \, L_k W_k / S \quad (7)$$

Because the classes of observed tornadoes are discrete the corresponding integral probability is not uniquely determined, and it assumes n_k values for a fixed class k:

$$F_i \, (k) = \begin{cases} \dfrac{i \alpha_0 L_0 W_0}{S} & \text{при } k = 0 \; (i = 1, \ldots \, n_0) \\[2ex] \dfrac{1}{S} \sum_{j=0}^{k-1} n_j \alpha \, (j) \, L_j W_j + \dfrac{i \alpha \, (k) \, L_k W_k}{S} & \text{при } k > \end{cases}$$

$$0 \; (i = 1, \ldots \, n_k) \quad (8)$$

We note that the method for determining the expected characteristics of tornadoes employed in the USA as a basis for regional tornado criteria to be used in designing NPP[10] is predicated on the assumption that the tornado-passage area does not depend on the tornado intensity. The characteristic tornado-passage area is established based on the estimate obtained in [11] from data on tornadoes recorded in the states of Iowa and Kansas. Since the dependence of the tornado-passage area on the tornado intensity is strong, this approach underestimates the expected loads.

A graph of the curve of the integral probability is best constructed using a scale for F(k) that gives a more or less straight line for the system of empirical points. Since the tornado-passage area is a power-law function of the tornado class, it can be assumed that a satisfactory straight line for the empirical curve can be obtained with a logarithmic probability scale. In this case

$$-\ln F(k) = ak + b \quad (9)$$

where a and b are constants determined by the method of least squares:

$$a = \frac{\langle k \rangle \langle \ln F(k) \rangle - \langle k \ln F(k) \rangle}{\langle k^2 \rangle - \langle k \rangle^2}$$

$$b = \frac{\langle k \rangle \langle k \ln F(k) \rangle - \langle k^2 \rangle \langle \ln F(k) \rangle}{\langle k^2 \rangle - \langle k \rangle^2} \qquad (10)$$

In the expressions (10) the symbol less than. greater than denotes averaging.

$$\langle x \rangle = \frac{1}{n} \sum_{m=1}^{n} x_m$$

where

$$n = \sum_{k=0}^{\ell} n_k$$

is the number of tornadoes observed in the region.

The area threshold probability P_O that a tornado affects one reactor per year, above which the possibility of the passage of a tornado through the site of an NPP must be taken into account, should be set at a quite low value so that the NPP can be reliably protected from possible accidents. In this paper the expert estimate of P_O is taken to be 10^{-7}. The same threshold probability is adopted in the USA [4, 10] and other member countries of IAEA [7].

The expected intensity class of a tornado that gives a probability P_O is determined from the condition

$$F(k_p) = 1 - P_O/P_s = 1 - P_O AT/S \quad (11)$$

It follows from (9) and (11) that

$$k_p = -\frac{1}{a}\left[\ln\left(1 - \frac{P_0 AT}{S}\right) + b\right] \qquad (12)$$

The expected characteristics of a probable tornado—the rotational velocity of the funnel wall, the translational velocity of the tornado, and the pressure drop between the periphery and the center of the funnel—are given by the formulas:

$$V_p = 6.3 \, (k_p + 2.5)^{1.5} \text{ m/sec}$$

$$U_p = 1.575 \, (k_p + 2.5)^{1.5} \text{ m/sec} \quad (13)$$

$$\Delta P_p = \rho V_p^2 = 0.486 \, (k_p + 2.5)^3 \text{ gPa}$$

where $\rho = 1.225 \text{ kg/m}^3$ is the standard density of air.

The data on overland tornadoes in USSR in the period 1844-1986, taken from [5] (241 cases) and supplemented by M. Ye. Lyakhov (19 cases), served as the starting point for determining the expected characteristics of probable tornadoes. These data, classified based on the intensity scale, are inhomogeneous, because the observations were made during different periods and the tornadoes in different regions were not recorded with the same degree of completeness.

Tornadoes assigned in [5] to an intermediate class were given a corresponding median fractional class, employed together with integer classes in the calculations.

The territory of the USSR was divided into regions with different tornado intensities and probabilities by means of statistical-genetic analysis of the starting characteristics of the tornadoes. The spatial uniformity of the statistical estimates of tornado recurrence was established taking into account the climatic regionalization, presented in [6], of the territory of the USSR for construction.

The classifications made gave 16 regions with different tornado intensities and probabilities; the regions were characterized by the spatial uniformity of climatic conditions for tornado formation (Fig. 2). The starting data for probabilistic estimates of the expected characteristics of tornadoes (areas of regions, effective observational periods, the coefficients α_O and the distribution of tornadoes over the intensity classes), presented in Table 1, were established for each region. We note that the exponential growth of the tornado-passage area as a function of the tornado class is responsible for the negligibly small computational errors arising from the choice of α_O for regions in which tornadoes of class 2 and higher were recorded. Two hundred sixty tornadoes were recorded within the separate regions.

In dividing the territory of the USSR based on the effects of tornadoes it was established that there are no significant contrasts in the statistical estimates of the expected characteristics of probable tornadoes, obtained for tornado zones (see Fig. 1) and for large regions containing these zones. Tornado zones were not included at this stage in the regionalization system in order to avoid spatial detailing of the field of expected characteristics that is not justified by the starting data. However, the tornado probability for separate sections and differences within regions were also calculated.

The probabilities P_S were calculated for separate regions; they turned out to be higher than the area threshold probability in only nine regions. Two hundred thirty-seven tornadoes were observed in them (91 percent of all tornadoes recorded in the USSR). Calculations were performed in an analogous manner for tornado zones in which 181 tornadoes were recorded (70 percent of the total number of recorded tornadoes). The computed characteristics of tornadoes were determined for each of
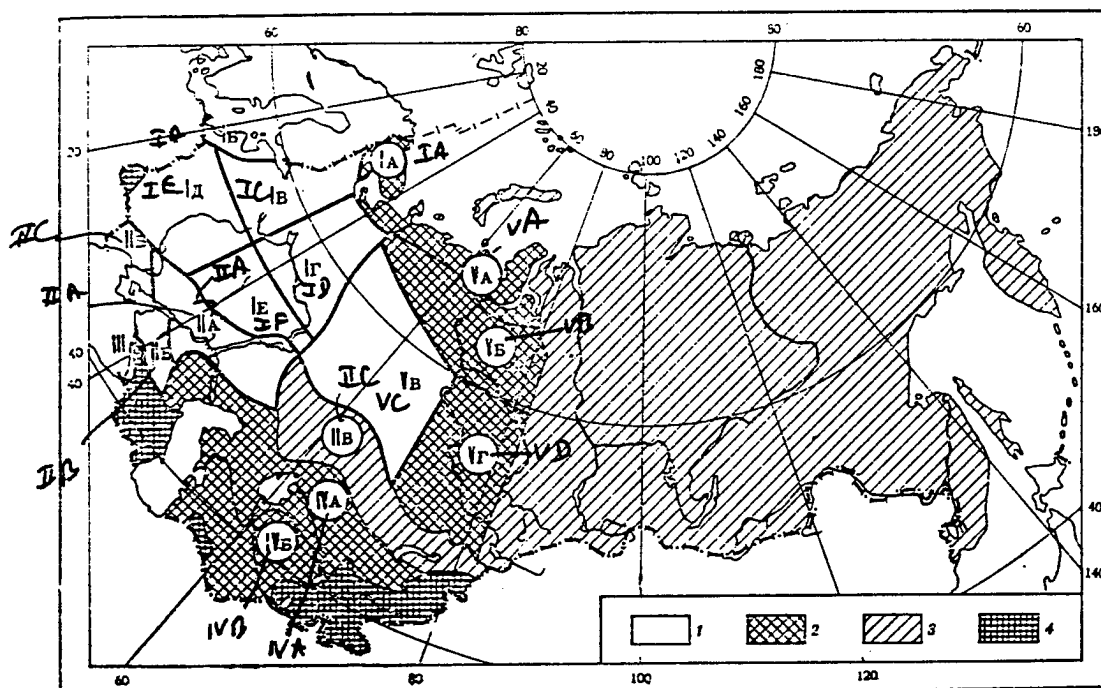
Figure 2. Division of the Territory of the USSR Into Regions Based on Tornado Intensity and Probability. 1—P_S greater than P_O; 2—O less than P_S less than P_O; 3—regions in which tornadoes have never been recorded; 4—little-studied regions. The starting data and the expected characteristics of tornadoes by region and tornado zones are taken from Tables 1 and 2.

the nine indicated regions and tornado zones: the intensity class, the rotational velocity of the funnel wall, the translational velocity, and the pressure drop between the periphery and the center of the funnel (see Table 2). In the rest of the USSR the following regions

were separated in accordance with the adopted regionalization based on tornado intensity and probability: regions with probability P_S less than the threshold (P_S less than 10^{-7}); region sin which tornadoes have thus far never been recorded; and, little-studied regions.

Table 1. Starting Data on Tornadoes Based on Regions and Tornado Zones

Region (zone)	A, 1000 km²	T, years	α_o	Tornado distribution over intensity class									Number of tornadoes in the region (zone)
				0	0.5	1	1.5	2	2.5	3	3.5	4	
						By Regions							
IA	197	20	4	1	-	-	-	-	-	-	-	-	1
IB	60	20	2	2	-	1	-	-	-	-	-	-	3
IC	525	20	2	4	3	4	5	2	-	-	-	-	18
ID	668	62	1.5	7	-	8	-	9	1	5	1	1	32
IE	700	47	1.5	15	-	26	-	13	-	4	-	-	58
IF	414	45	2	12	-	17	1	1	-	4	-	-	32
IIA	534	26	3	3	-	8	-	7	-	-	-	-	18
IIB	206	28	1.5	17	-	11	-	2	1	1	-	-	32
IIC	970	-	-	-	-	-	-	-	-	-	-	-	-
III	7	34	1.5	17	-	2	-	-	-	-	-	-	19
IVA	1044	26	4	2	-	-	-	1	-	-	-	-	3
IVB	819	26	3	4	-	1	-	-	-	-	-	-	5

VA	510	26	4	2	2	-	-	-	-	-	-	-	2
VB	842	30	4	1	-	2	-	1	-	-	-	-	4
VC	1498	53	3	2	-	13	1	9	-	-	-	-	25
VD	1037	26	4	1	-	7	-	-	-	-	-	-	8

By Tornado Zones

A	376	38	1.5	12	3	30	4	13	1	3	-	-	66
B	494	44	1.5	26	-	26	1	12	1	8	1	1	76
C	39	32	1.5	21	-	7	-	-	-	-	-	-	28
D	96	31	2.0	1	-	7	-	3	-	-	-	-	11
A-F	229	28	1.5	9	3	19	4	11	-	2	-	-	48
A-FS	78	41	1.5	1	-	3	-	1	-	1	-	-	6
A-S	69	34	1.5	2	-	8	-	1	1	-	-	-	12
B-F	202	64	1.5	8	-	6	1	7	-	7	1	1	31
B-FS	152	39	1.5	6	-	13	-	-	-	-	-	-	19
B-F	140	30	1.5	12	-	7	-	5	1	1	-	-	26

Table 2. Expected Characteristics of Tornadoes by Regions and Tornado Zones

Region (zone)	$P_S \cdot 10^7$ yr-1	$P_o = 10^{-7}$, yr-1				$P_o = 10^{-6}$, yr-1			
		k_p	v_p, m/sec	u_p, m/sec	Δp_p, gPa	k_p	v_p, m/sec	u_p, m/sec	Δp_p, gPa
By Region									
IB	1.64	0.56	34	8	14	-	-	-	-
IC	3.63	1.75	55	14	37	-	-	-	-
ID	38.6	3.69	97	24	115	3.57	94	24	108
IE	14.2	2.75	76	19	70	2.21	64	16	51
IF	6.57	2.12	62	16	48	-	-	-	-
IIA	5.60	2.01	60	15	44	-	-	-	-
IIB	24.2	2.71	75	19	69	2.44	69	17	59
III	19.1	1.07	43	11	22	0.61	34	9	15
VC	1.37	1.47	50	12	30	-	-	-	-
By Tornado Zone									
A	29.9	2.58	72	18	64	2.41	69	17	58
B	87.2	3.58	94	24	109	3.52	93	23	106
C	8.95	1.18	44	11	24	-	-	-	-
D	12.2	1.93	59	15	42	1.19	45	11	24
A-F	45.2	2.53	71	18	62	2.43	69	17	58
A-FS	29.4	2.89	79	20	76	2.71	75	19	69
A-S	18.8	2.14	63	16	49	1.82	57	14	39
B-F	133	3.75	98	25	119	3.72	98	24	117
B-FS	2.82	1.10	43	11	23	-	-	-	-
B-S	37.8	2.81	77	19	73	2.66	74	18	67

For comparison Table 2 also gives the corresponding expected characteristics calculated with $P_O = 10^{-6}$. The tornado-passage probabilities exceed this level only in four regions: ID, IE, IIB, and III. On the section B-L of zone B the probability P_S exceeds 10^{-5}.

The exponential character of the integral empirical curve of the class distribution of tornadoes leads to the fact that significant variations of the probability P_S with $P_O = 10^{-7}$ do not significantly affect the expected characteristics. In addition, the expected class of a tornado is close to the maximum observed class. The calculations show that increasing or decreasing P_S by a factor of 3-5 correspondingly increases or decreases the expected class by not more than 0.1-0.3.

The example of the empirical distribution of the tornado-intensity class and its approximation on a logarithmic probability scale for region IC presented in Fig. 3 as well as the results of calculations based on the other eight regions and four tornado zones agree satisfactorily with an exponential empirical class distribution of tornadoes.
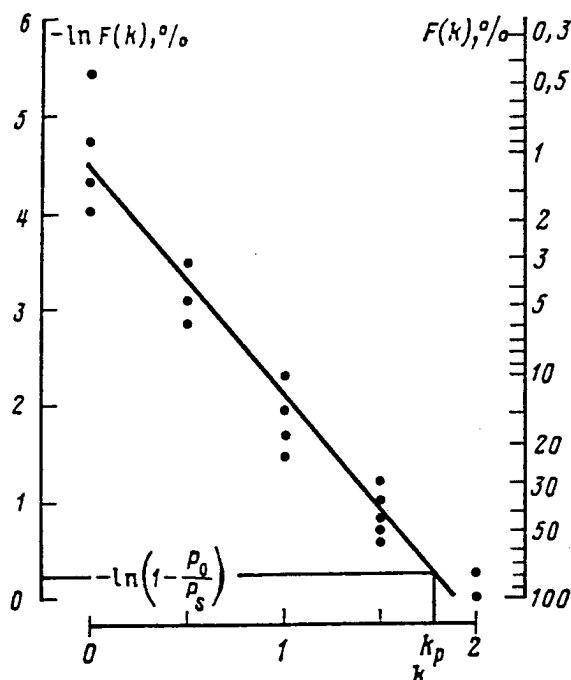
Figure 3. Empirical Integral Distribution of Tornado-Intensity Classes on a Logarithmic Probability Scale. Region IC.

It is obvious that the expected class of a tornado is determined primarily by the maximum observed class. The results of calculations over all regions indicate that k_p is highly stable, and therefore v_p, u_p, and Δp_p depend on the region P_O/P_S for P_S more than P_O.

The probability estimates, presented in this paper, of tornado characteristics can be employed for siting NPP. For site selection and subsequent stages in the design of NPP an additional analysis of the statistics of tornadoes taking into account the physical-geographic and climatic conditions of tornado formation should be performed. The expected characteristics of tornadoes should be estimated at these stages taking into account additional information of the passage of tornadoes in the region where the NPP is to be constructed and the existence of tornado zones.

Conclusion

1. The yearly tornado-passage probabilities vary over a wide range. Over a significant part of the European Territory of the USSR they exceed 10^{-7}, the threshold at which they are customarily taken into account in designing NPP, and can reach 10^{-5} locally in tornado zones. The correlation between tornado zones in the European Territory of the USSR and the prevailing position of atmospheric fronts indicates that tornadoes are genetically related with the passage of fronts.

2. The empirical integral distributions of tornadoes over intensity classes are satisfactorily described by an exponential law. The expected characteristics of tornadoes are largely determined by the maximum observed intensity class.

3. A method was proposed for determining the expected characteristics of tornadoes in a region where a nuclear power plant is to be constructed. The territory of the USSR was divided into regions according to tornado intensity and the tornado-passage probability using this method. The basic expected characteristics of probable tornadoes were determined for each region: the passage probability, the intensity class, the rotational velocity of the funnel wall, the translational velocity, and the pressure drop between the periphery and the center of the funnel.

References

1. Atlas of the USSR, Chief Directorate of Geodesy and Cartography, Moscow (1983).

2. Lyakhov, M. Ye., "Tornadoes in the Central Belt of Russia," IZV. AKAD. NAUK SSR, SER. GEOGR., No. 3, pp 67-72 (1986).

3. Nalivkin, D. V., "Uragany, buri, i smerchi. Geograficheskiye osobennosti i geologicheskaya deyatelnost (HURRICANES, STORMS, AND TORNADOES. GEOGRAPHICAL CHARACTERISTICS AND GEOLOGICAL ACTIVITY), Nauka, Moscow (1969).

4. Simiu, E. and Skanlan, R., Vozdeystviye vetra na zdaniya i sooruzheniya (EFFECT OF WIND ON BUILDINGS AND STRUCTURES), Stroyizdat, Moscow (1984).

5. Snitkovskiy, A. I., "Tornadoes on the territory of the USSR," METEOROLOGIYA I GIDROLOGIYA, No 9, pp 12-25 (1987).

6. Building Standards and Regulations. Building Climatology and Geophysics. Building Standards and Regulations 2.01.01-82, Stroyizdat, Moscow (1983).

7. "Making allowances for external meteorological phenomena when siting nuclear power plants (neglecting tropical cyclones)," IAEA, Series of Publications on Safety, 1983, No 50-SG-SIIA.

8. Dergarabedian, P. and Fendell, F., "Estimation of maximum wind in tornadoes," TELLUS, Vol 22 No 5, pp 511-516 (1970).

9. Fujita, T. T., "Tornadoes and downbursts in the context of generalized planetary scales," J. ATM. SCI., Vol 38, No 8 pp 1511-1534.

20

10. Markee, E. H., Beckerley, J. G., and Sanders, K. E., "Technical basis for interim regional tornado criteria," WASH-1300, U.S. Atomic Energy Commission (1974).

11. Thom, H. C. S., "Tornado probabilities," Mon. Weath. Rev., Vol 91, No 10-12, pp 730-736 (1963).

12. Pokrovskiy, O. M. "Optimizatsiya meteorologicheskogo zondirovaniya atmosfery so sputnikov" (OPTIMIZATION OF METEOROLOGICAL SOUNDING OF THE ATMOSPHERE FROM SATELLITES), Gidrometeoizdat, Leningrad (1984).

Power Plants Abstracts

*18610398c Moscow ELEKTRICHESKIYE STANTSII
in Russian No 2, Feb 89 pp 95-96*

[Abstracts of articles appearing in "Power Plants", 1989]

[Text]

UDC 621.311.072.8

Ways of Covering Semipeak Zone of Load Graph and Assessing Their Efficiency in Future. I. A. Alekseyev and G. I. Samorodov, pp 2-7

A method of assessing the efficiency of covering the semipeak portion of future load graphs of the country's European regions is proposed.

This article presents comparative results of an evaluation of different versions of covering the semipeak zone of load graphs for the country's European regions. It is shown that using ultralong electric power lines to connect Siberia's GES for these purposes is more effective than is constructing complexes of AES, semipeak GAES, and demand-adaptable KES in the European regions.

UDC 621.316.728.016.24

Features of Automatic Limitation of Overcurrents in South's United Power Generation System. S. A. Molkov, pp 10-12

This article examines the difficulties in automatically limiting overcurrents in the South's United Power Generation System under modern conditions. To overcome these difficulties, principles have been proposed for coordinating the automatic frequency and active power regulation system of the Southern United Power Generation System with the accident prevention automation equipment of the Southern United Power Generation System and the automatic frequency and active power regulation system at the level of the USSR Unified Power Generation System, which may also be useful in developing automatic frequency and active power regulation systems for other transit United Power Generation Systems. References 8.

UDC 621.311.016.25.07

Degree of Compensation for Load Capacity of High-Voltage Lines. V. A. Chevychelov, pp 13-17

This article presents the results of research to determine the requirements with regard to the degree of compensating for the load capacity of the power lines from electric power plants that are commutated at a voltage of 500 kV or higher based on limiting the discharge of reactive power to the electric power plants generators. References 4.

UDC 621.182.23.004.76

Combined/Separate Burning of Blast Coke and Natural Gases in PK-14-2 Boiler. A. F. Bogatyrev, M. A. Bukhman, B. R. Chudovskiy, and S. A. Makhmudov, pp. 20-25

This article describes the results of developing and studying a full-scale prototype of a multifuel straight flow-swirl burner device that is intended for combined/separate burning of natural, coke, and blast furnace gases in a PK-14-2 boiler at the Magnitogorsk Metallurgical Combine.

Research and industrial test results have established that the burner device provides aerodynamic self-regulation of the flame's position when there is a change in the thermal percentage of blast furnace gas. It also ensures corresponding changes in the heat reception of the superheater, separation of the initial combustion sections, and consequently, elimination of the neutralization of the natural and coke gas flames by the blast furnace flame. The burnup of the fuels (at all ratios of fuels in the mixture) ends inside the furnace compartment, and there is no chemical incomplete combustion once the air surplus coefficient is greater than or equal to 1.05. The emission of nitrogen oxides in the operating range of fuel ratios is between 70 and 250 mg/m^3.

The burners operate reliably and provide stable fuel ignition and combustion with regulation of the air flow rate only by a ventilator guide independently of the fuel consumption ratio.

The anticipated savings from introducing the burner devices in one boiler amount to about 500,000 rubles. References 5.

UDC 621.311.22:662.96.001.24

Allowing for Fractional Composition of Ash When Calculating Its Ground Concentrations. A. K. Vnukov and F. A. Rozanova, pp 23-28

This article presents a method of calculating the value of the sedimentation coefficient F as a function of the fractional composition of ash that meets the requirements specified in OND-86. The fractional composition, terminal velocity values, and sedimentation coefficient are presented for a number of types of coals and ash removers. References 5.

UDC 621.165.001.42.004.17

Estimating Economy of K-210-130 Turbine Plants at Leningrad Metal Plant imeni 22nd CPSU Congress. G. V. Rupakov, V. P. Rubtsov, and T. D. Dzhumatayev, pp 28-33

This article presents the technical and economic indicators of two K-210-130 turbine plants at the Leningrad Metal Plant imeni 22nd CPSU Congress. The indicators were obtained from routine tests. From the standpoints of both volume and precision level, the characteristics obtained are fully adequate to verify the conformity of the turbine plants' actual indicators to data on standard power generation characteristics. References 6.

UDC 621.621.165-23.21

Diagnosing Condition of Turbine Set Bearings Based on Purity of Oil in Oil Supply System. I. F. Pshenisnov and Ya. I. Pshenisnov, pp 34-36

A method of making an express analysis of the purity of turbine oil has been developed. Research has been conducted on the contamination of oil in the oil supply systems of domestic turbine sets, and existing detergents have been analyzed. It has been demonstrated that a granulometric analysis of contaminants at different points in an oil supply system may be used to make a technical diagnosis of the condition of turbine sets' bearings. References 6.

UDC 621.182.44.004

Hydrolicity of SKD Power-Generating Units After Steam and Oxygen Passivation. N. N. Mankina, B. S. Fedoseyev, and A. A. Grishin, pp 36-42

This article presents data on the water and chemical regimens of T-250 power-generating units with periodic oxygen dosage after preliminary steam and oxygen passivation. It is shown that there is no transfer of corrosion products in the power-generating unit's steam and water cycle. The possibility of eliminating equipment conservation measures when the equipment is shut down for extended periods is established, and the periodicity and duration of the oxygen dosage is determined.

UDC 621.311.002.51.001.4:621.313.333.2

Operation of Nuclear Power Plant With Transverse Water and Steam Connections During Interruption in Auxiliary Feed. V. Kh. Georgiadi and N. V. Kholshcheva, pp 42-48

This article discusses the results of an experimental verification of the operation of the primary equipment at a nuclear power plant with transverse water and steam connections during interruptions in the auxiliary feed. The makeup of the auxiliary electric drives participating in the self-triggering is presented. It is shown that, given the existing design of the electrical power supply of the electric motors of the oil pumps used to lubricate the electric feed pumps and the online alternating current circuits of the main vessel, disconnections of the electric feed pumps will always occur when there are interruptions in the feed. Recommendations are given for increasing the operating reliability of electric feed pumps

during interruptions in the auxiliary feed, and it is demonstrated that an interruption of the power supply to the auxiliary electric drives of as much as 6 to 7 seconds is permissible when taking the measures.

UDC 621.181.23.004

Experience of Operating System To Automatically Monitor Technical Condition of GT-35 Gas Turbine Plants of PGU-250 Steam and Gas Units. A. I. Mexhanikov, V. I. Akhrameyev, S. V. Maksimov (deceased), I. L. Shvartsenberger, V. A. Yeremenchuk, and Yu. A. Martynenko, pp 48-54

This article analyzes the technical condition of a gas turbine plant during the process of its extended operation based on the results of periodic thermal tests and data obtained by using an automated monitoring system. The errors in determining the overall indicators of the gas turbine plant's condition are calculated, and the stability of their deviations from the mean values are estimated. Recommendations are provided for improving the system to monitor the gas turbine plant. References 2.

UDC 621.182-5.001.572

Analytical Investigation of System To Regulate Feed of P-67 Boiler. V. I. Vasilyev, pp 54-59

This article examines the results of digital computer studies of the dynamics of two versions of an automatic feed regulation system that has signals to indicate "heat" and a temperature beyond the VRCh [not further identified] and that uses structural-type linear mathematical models directly in a time interval.

Parameters for adjusting the two versions of the automatic regulation system were selected on the basis of the boiler's dynamic characteristics that were obtained in models, and they were compared during characteristic perturbations. Recommendations are given concerning the adjustment parameters of automatic regulation systems for practical adjustment on operating equipment. References 5.

UDC 621.311.22:681.5

Using Microprocessors for Local Automation of Production Processes at TES. Ye. A. Shelkov, pp 59-63

Problems in using microprocessor technology in power generation are examined. Based on the example of a device to monitor the vacuum in a turbine condenser, a method is shown for developing microprocessor devices to perform local tasks related to automating production processes. It is shown that using microprocessors makes it possible to successfully perform automation, monitoring, and control tasks that are not accessible to traditional automation equipment. The existing lag of power generation in this field of technology is covered.

UDC 621.311-544:621.316.728.016.24

Using Transfer of GES Units to Generator Mode in Automatic Regulation of Frequency and Active Power, A. G. Batalov, A. N. Molkov, and S. A. Molkov, pp 63-66

This article is devoted to the problems of increasing the effectiveness of the hierarchical automatic frequency and active power regulation system of the USSR Unified Power Generation System. It is proposed that the automatic transfer of GES units into a generator mode based on instructions from the automatic frequency and active power regulation system at the United Power Generation System level be used under conditions of inadequate regulation ranges. It is proposed that the technological algorithm, which may be implemented in the existing automatic frequency and active power regulation system at the United Power Generation System level, be corrected to adapt to delays in working out control actions arising in such a case. References 9.

UDC 621.313.322-82.016.313.001.4

Asymmetrical Load Mode of Hydraulic Turbine Generators With Direct Water Cooling of Copper Stator. G. N. Ter-Gazaryan, S. S. Ananyants, and Ya. G. Bidzhamov, pp 71-74

This article examines the results of full-scale studies of an asymmetrical load mode of high-power hydraulic turbine generators with direct cooling of their stator winding. It is shown that heating the poles with a reverse-synchronous field does not limit the current of the inverse sequence that is permissible for long periods within the bounds necessary for using the output of a portion of the power of the GES unit through two transformer phases. The current of the inverse sequence that is permissible for long periods is limited by the vibration stability of portions of the generator during the

effect of forces pulsing with a frequency of 100 Hz. Based on this criterion, the current $I_2 = 0.1$-$0.13/N$ (which is significantly higher that the GOST-specified regulation value for hydraulic turbine generators) is permissible for long periods.

UDC 621.313.323:621.316.9

Protecting Synchronous Electric Motors From an Asynchronous Mode. V. F. Sivokobylenko and A. V. Levshov, pp 75-80

This article examines the pulse protection of synchronous electric motors against an asynchronous mode. The protection is based on controlling the phase angle between the current and voltage of the stator. It is included in the automatic resynchronization circuit. Block diagrams and technical characteristics are presented. Small-series production has been initiated. The operating experience has been positive. References 6.

UDC 621.313.322-81:621.316.925

High-Speed Device To Detect Asynchronous Mode During Loss in Excitation of High-Power Turbogenerators. G. M. Pavlov, S. B. Vorokhobin, K. N. Semenov, and A. I. Tadzhibayev, pp 80-84

This article presents the results of studies of the modes during an excitation loss as well as modes with the excitation of modern high-power turbogenerators. The possibility is demonstrated of increasing the selectivity and speed of protection against an asynchronous mode based on the use of a special algorithm for the functioning of the measuring-logic portion of the protection. A diagram of the device for detecting an asynchronous mode of a high-power turbogenerator is presented. References 10.

T-50-130-6 Steam Extraction Turbine

18610398a Moscow ELEKTRICHESKIYE STANTSII in Russian No 2, Feb 89 p 93

[Text] The T-50-130-6 steam extraction turbine has been offered for licensing. It has a condensation unit and two regulatable heating steam bleeds and is intended to directly drive a generator and heat release for heating purposes.

The turbine makes it possible to produce electric and thermal power more economically. It has two regulatable heat bleeds, an upper one and a lower one, that are intended to gradually heat network water.

The turbine can operate with two regulatable steam bleeds or the one lower one, or it can operate in a purely condensation mode with the bleeds switched off, which affords the capability of operating the turbine optimally under different conditions.

The automatic regulation, protection, and alarm system is designed to be connected up or to function as a stand-alone unit with hydraulic transfer connections.

The T-50-130-6 turbine's high specific production of electric power based on heat consumption provides the following:

high live steam parameters;

an advanced system for the regenerative heating of feed water;

use of gradual heating of network water;

a low pressure level of the steam directed to the heating bleeds;

specially designed turbine setting intended for use under conditions of operation with heating networks.

The following are the turbine's technical characteristics:

Capacity, MW:	
Rated	50
Maximum	60
Rotation frequency, s^{-1}	60
Live steam pressure, MPa	12.8
Live steam temperature, °C	555
Thermal load of heating bleeds, GJ/j	377
Limits of pressure change in regulatable steam bleeds, MPa:	
Upper	0.059-0.245
Lower	0.049-0.196

The turbine and the equipment supplied with it contain 12 inventions that have a positive effect on its key technical and economic parameters.

The "know-how" and "engineering"-type services as well as the necessary documentation have been offered for licensing.

©Energoatomizdat, "Elektricheskiye stantsii", 1989

R-102/107-130/15-2 Steam Extraction Turbine

18610398b Moscow ELEKTRICHESKIYE STANTSII in Russian No 2, Feb 89 p 94

[Text] The R-102/107-130/15-2 steam extraction turbine with counterpressure has been offered for licensing. It is intended to directly drive a generator and heat release for industrial purposes.

The R-102/107-130/15-2 turbine is the largest turbine in the world with counterpressure that discharges steam for industrial purposes.

The turbine is an 11-cylinder set. The cylinder is a double-walled counterflow cylinder. The turbine has nozzle steam distribution that is implemented by four actuator valves.

The turbine is equipped with an electrohydraulic automatic regulation system that is intended to maintain it within specified limits depending on the turbine's operating mode and the rotation frequency of the turbogenerator's rotor, the turbogenerator's electric load (capacity), and the steam pressure beyond the turbine.

In the event of an instantaneous discharge of the electrical load from the generator, the hydraulic portion of the regulation system limits the increase in the rotation frequency of the turbogenerator's rotor below the level at which the safety automation equipment requires adjustment.

The turbine is equipped with monitoring, alarm, and remote control systems that make it possible to start, stop, and control an operating turbine from a remote panel.

The regenerative unit is intended to heat the feed water by steam that has been extracted from the counterpressure and the turbine's uncontrolled bleeds and includes three high-pressure heaters and pipelines with a fitting.

Operating experience has confirmed the high economy, demand adaptability, and operating reliability of the R-102/107-130/15-2 turbine. Its technical characteristics are as follows:

Capacity, MW:	
Rated	102
Maximum	107
Rotation frequency, s^{-1}	50
Live steam pressure, MPa	12.8
Live steam temperature, °C	555
Range of change in steam pressure beyond the turbine (counterpressure), MPa	1.18-20.6
Live steam flow rate, t/h	782
Rated flow rate of steam into counterpressure line, t/h	670

The turbine's design includes eight inventions that have a positive effect on its key technical and economic parameters, as is confirmed by the industrial prototype.

The "know-how" and "engineering"-type services as well as the necessary documentation have been offered for licensing.

UDC 531.8

Some Tasks in Researching Vibrations of Industrial Robot Arm Based on Mechanical Models of It

18610402a Moscow IZVESTIYA VYSSHIKH UCHEBNYKH ZAVEDENIY: MASHINOSTROYENIYE in Russian No 12, Dec 88 pp 29-33

[Article by V. N. Vernigor, candidate of physical and mathematical sciences and docent, and V. A. Gurevich, engineer; first paragraph is IZVESTIYA VYSSHIKH UCHEBNYKH ZAVEDENIY: MASHINOSTROY-ENIYE abstract]

[Text] Mechanical systems with a finite number of degrees of freedom that describe the vibrations of the grip of an industrial robot's arm as it turns under the effect of a random rotating force are derived. These mechanical models are used as the basis for solving the problem of the grip's vibrations when the arm turns with an allowance for the braking moment and the arm's repeated collisions against a rigid stop. The problem of the optimum parameters of the turning drive and braking devices is also solved.

In problems of optimizing the design parameters of an industrial robot's arm and its braking devices it is necessary to make an allowance for the elasticity of the manipulator's links. We will examine the arm vibrations of type RF-201, universal-5, and tsiklon-3B industrial robots that arise when the arm is turned.
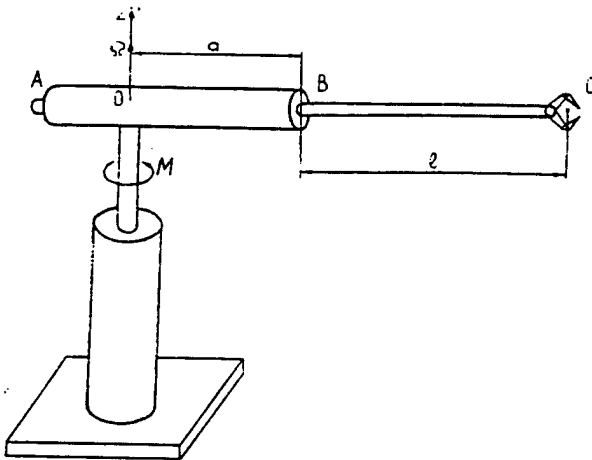

Figure 1

Let the manipulator's arm turn under the effect of the rotary moment M = M(t). The manipulator's boom BC (Figure 1) will be considered an elastic rod with the length l, at point C of which the mass m of the gripper

and the load being moved is concentrated. The arm's cylinder AB will be assumed to be an absolutely solid body. The problem of the vibrations of the manipulator's boom is reduced to the integration of a system of differential equations[1]

$$I_1 \frac{d\overline{\Omega}}{d\overline{t}} + \int_0^1 \left[(\overline{a}+\overline{x}) \frac{d\overline{\Omega}}{d\overline{t}} + \frac{\partial^2 \overline{y}}{\partial \overline{t}^2} \right] (\overline{a}+\overline{x}) d\overline{x} + \overline{m} \times$$

$$\times \left[\frac{\partial^2 \overline{y}(1,\overline{t})}{\partial \overline{t}^2} + (\overline{a}+1) \frac{d\overline{\Omega}}{d\overline{t}} \right] (\overline{a}+1) = \overline{M} \qquad (1)$$

$$\frac{\partial^2 \overline{y}}{\partial \overline{t}^2} + \frac{\partial^4 \overline{y}}{\partial \overline{x}^4} = -(\overline{a}+\overline{x}) \frac{d\overline{\Omega}}{d\overline{t}}$$

given the boundary conditions

$$\overline{y}(0, \overline{t}) = 0, \quad \frac{\partial \overline{y}}{\partial \overline{x}}\Big|_{\overline{x}=0} = 0, \quad \frac{\partial^2 \overline{y}}{\partial \overline{x}^2}\Big|_{\overline{x}=1} = 0,$$

$$\frac{\partial^3 \overline{y}}{\partial \overline{x}^3}\Big|_{\overline{x}=1} = \overline{m} \left\{ \frac{\partial^2 \overline{y}}{\partial \overline{t}^2}\Big|_{\overline{x}=1} + (\overline{a}+1) \frac{d\overline{\Omega}}{d\overline{t}} \right\}, \qquad (2)$$

where $x = x/l$, $y = y/l$, $a = a/l$, t = the square root of c_* times t divided by M_1, $m = m/m_1$, $I_1 = I_1/M_1 l^2$, = Ω times the square root of M_1 divided by the square root of c_*, $M = M/c_* l^2$, $c_* = EI/l^3$, $M_1 = \rho Sl$ is the mass of the boom without the gripper, E is the Young modulus, ρ is the density, I is the inertial moment of the cross section, S is the area of the cross section, a is the distance from the beginning of the boom to the rotation axis, O is the angular velocity of the column, I_1 is the inertial moment of the cylinder and the column relative to the rotation axis, y is the flexure of the boom, and x is the coordinate of the cross section.

Integrating differential equation system (1) given complex laws governing the change in rotary moment M = M(t) causes great problems. We will represent the manipulator's boom as an elastic weightless rod EF with the concentrated masses $m_1^{(n)}$, $m_2^{(n)}$, ..., $m_n^{(n)}$, which are a distance of $l_1^{(n)}$, $l_2^{(n)}$, ..., $l_n^{(n)}$, respectively, away from the beginning of the boom. We will assume that the distance from the beginning of the rod to the rotation axis OZ equals $a^{(n)}$ and the inertial moment of the cylinder DE relative to the rotation axis equals $I_1^{(n)}$ (Figure 2). We will assume that the rotary moment M = M(t) is applied to the weightless axis GS, which is connected with the cylinder DE by a spring with the stiffness $c_0^{(n)}$. We will view the displacement of the mass $m_1^{(n)}$ relative to the axis GS as the flexure of the robot's arm at the point of the gripper.

We will determine the values $a^{(n)}$, $I_1^{(n)}$, $m_1^{(n)}$, ..., $m_n^{(n)}$, $l_1^{(n)}$, ..., $l_n^{(n)}$ by examining the dynamic compliance R(o) of the robot's arm at the point of the gripper and the
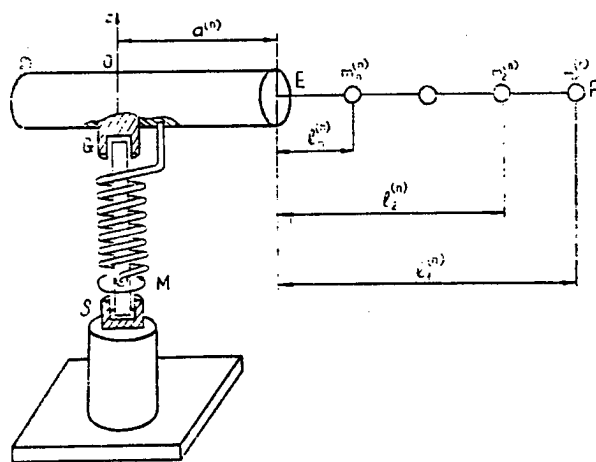
Figure 2

dynamic compliance $R_1(o)$ of the rod at the point where the mass $m_1^{(n)}$ is located.[2] If the dynamic compliance $R(o)$ is approximately represented in the form

$$\overline{R}(z) = -\frac{\overline{a}^{(n)} + \overline{I}_1^{(n)}}{\overline{c}_0^{(n)}} + \sum_{k=1}^{n} \frac{\overline{L}_k}{z_k^4 - z^4}, \quad \frac{\overline{a}^{(n)} + \overline{I}_1^{(n)}}{\overline{c}_0^{(n)}} =$$

$$\sum_{k=1}^{n} \frac{\overline{L}_k}{z_k^4} - \overline{R}(0), (3)$$

then, the following conditions will be sufficient to satisfy the identity $R(z)$ is identical to $R_1(z)$: $z_{1k} = z_k$, $L_{1k} = L_k$ (k=1, 2, ..., n), (4)

where $R(z) = EIR(o)/l^2$, $R(z) = EIR_1(o)/l^2$, z = the square root of o times l divided by α, $\alpha^4 = EI/\rho S$, $c_0^{(n)} = c_0^{(n)}/c_* l^2$, $a^{(n)} = a^{(n)}/l$, $l_k^{(n)} = l_k^{(n)}/l$, $L_k = L_k M_1 l$, $L_{1k} = L_{1k} M_1 l$, z_k = the square root of o_k times l divided by α, z_{1k} = the square root of o_{1k} divided by α, L_k is the arm's total length corresponding to its natural vibration frequency o_k, and L_{1k} is the total length of the rod EF corresponding to its natural vibration frequency o_{1k}. Conditions (4) may be viewed as a system of algebraic equations relative to the known parameters $a^{(n)}$, $l_k^{(n)}$, $I_1^{(n)} = I_1^{(n)}/M_1 l^2$, $m_k^{(n)} = m_k^{(n)}/M_1$, (k = 1, 2, ..., n).

Conditions (4) mean that, when determining the flexure of the arm y(l, t) based on the specified models in an expression for y(l, t) in the form of a series based on natural vibration forms derived from system (1) and boundary conditions (2), only the terms corresponding to the first n forms of the vibrations are considered. The remaining terms of this series are allowed for by introducing the additional rigidity $c_0^{(n)}$.

By integrating equation system (1) given boundary conditions (2) and $M = M_0 e^{j\omega t}$ along with the differential equation system describing the motion of the mechanical system depicted in Figure 2, we obtain an expression for the dynamic compliances $R(z)$ and $R_1(z)$. From these expressions we find the values that are required to determine the models' parameters

$$\overline{L}_k = 4z_k \left[\overline{a}z_k (\cos z_k + \operatorname{ch} z_k) + \sin z_k + \operatorname{sh} z_k - H(z_k) z_k (1 + \overline{a})\right] \times$$
$$\times \left\{2 [1 + \overline{a} + \overline{m} (1 - \overline{I}_1 z_k^4)] \sin z_k \operatorname{sh} z_k + z_k^2 [3\overline{I}_1 + 2\overline{a} (\overline{a} + 3\overline{am} + 2\overline{m})] \times\right.$$
$$\cos z_k \operatorname{ch} z_k + 3\overline{I}_1 z_k^2 + 2z_k [(1 + \overline{a} + 2\overline{m})\overline{a} + \overline{m}] (\cos z_k \operatorname{sh} z_k + \sin z_k \operatorname{ch} z_k) +$$
$$\left. + z^3 [\overline{I}_1 (1 + 4m) + 2\overline{a} \cdot \overline{m}] (\cos z_k \operatorname{sh} z_k - \sin z_k \operatorname{ch} z_k)\right\}^{-1},$$

$$H(z) = 1 + \cos z \operatorname{ch} z + \overline{m} z (\cos z \operatorname{sh} z - \sin z \operatorname{ch} z),$$

$$N(z) = z^3 H(z)\overline{I}_1 + 2\overline{m} z (\sin z + \overline{a} z \cos z)(\operatorname{sh} z + \overline{a} z \operatorname{ch} z) +$$
$$+ 2\overline{a} z \sin z \operatorname{sh} z + (z^2 \overline{a}^2 - 1)\cos z \operatorname{sh} z + (z^2 \overline{a}^2 + 1) \sin z \operatorname{ch} z.$$

$$\overline{R}(0) = -\frac{11 + 15\overline{a} + 40\overline{m}(\overline{a} + 1)}{40 [3\overline{I}_1 + 3\overline{a}^2 + 3\overline{a} + 3\overline{m}(\overline{a} + 1)^2 + 1]},$$

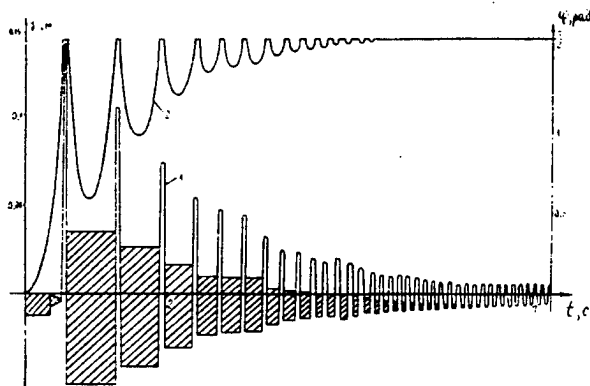where z_k are the roots of the frequency equation $N(z) = 0$.

The aforementioned has been a general method of constructing models of a robot's arm. In particular, for the case where n = 1, after transforms we obtain

$$\overline{a}^{(1)} = \overline{a}, \quad \overline{I}_1^{(1)} = 1, \quad \overline{I}_1^{(1)} = -\frac{\overline{a}+1}{\overline{L}_1},$$

$$\overline{m}_1^{(1)} = \frac{3}{z_1^4 + 3\overline{L}_1(\overline{a} + 1)}. \quad (5)$$

To estimate the errors arising when the mechanical models constructed are used, we use the results from a previous work[1] in which a solution y = y (l, t) was obtained for the second equation system (1) given O = const and specified design parameters of the robot's arm. By substituting the solution into the first equation system (1), we obtain the law $M = M_*(t)$ of the change in rotary moment governing the turning of the robot's arm at a specified constant angular acceleration. By integrating the equation system describing the motion of the mechanical system depicted in Figure 2, given $M = M_*(t)$ and the model parameters (5), we obtain an approximate expression for the flexure $y_*(t)$ of the arm at the point of the gripper. By comparing the curves of the functions y(l, t) and $y_*(t)$, we see that the precision of the solution obtained on the basis of the model of the arm constructed is completely sufficient for practical calculations. The maximum true relative error of the approximate solution, when $C_0^{(1)}$ = infinity, amounts to 2.2 percent. When $C_0^{(1)}$ is calculated in accordance with (3), it amounts to 0.035 percent.

The problem of the vibrations of an industrial robot's gripper was solved by way of an example based on a mechanical model of the arm corresponding to the case n = 1, $C_0^{(1)}$ = infinity. In Figure 3, curve 1 corresponds to

the law $y_1^{(1)}(t)$ of the motion of the gripper, and curve 2 corresponds to the law $\varphi = \varphi(t)$ governing the change in the arm's turning angle. When the arm turns at an angle of φ_0 (t_0 is applied to it. When φ_0)moment, the resistance moment $M_c = -b\varphi$ (caused by damping) is also applied. When $\varphi = \pi/2$ ($t = 0.49$ s), the arm collides against a rigid stop, after which it jumps back from the stop and collides with it once more. The rotary moment acting on the arm after the first collision was assumed to equal $M = M_0$; during the contact of the arm and stop, it was assumed that $\varphi = \pi/2$ and $\varphi^. = \varphi^{..} = 0$. The velocities during the collision were determined on the basis of elementary collision theory; during the collision, they were determined on the basis of Hertz's theory.[3] Between subsequent collisions of the arm against the stop, the gripper vibrates with a frequency of 32.4 Hz and a constant amplitude (in Figure 3 this amplitude corresponds to the striped regions). When t 5 s, it may be assumed that $\varphi = \pi/2$, $\varphi^.$ is identical with 0, and the gripper vibrates with a frequency of 9.4 Hz and constant amplitude. In the specified example, the manipulator's boom is a hollow cylinder with the length $l = 1$ m, the radii $r_1 = 0.013$ m and $r_2 = 0.015$ m, $a = 0.5$ m, $m = 5$ kg, $E = 200$ GPa, $\rho = 7,700$ kg/m^3, $I_1 = 0.3$ kg·m^2, $M_0 = 100$ N·m, $\varphi_0 = \pi/r$ rad, $b = 10$ kg·m^2/s, a recovery coefficient during impact of 0.556, an impact force relative to the arm's rotation axis of 0.25 m, a striker edge radius of 0.04 m, and a Poisson coefficient of 0.3. The design parameters of the manipulator's boom are taken from a previous work,[1] where the second equation system (1) is integrated for the specified law $O = O(t)$, which makes it possible to compare the solution of the specified problem in its various formulations.

Figure 3

The mechanical models of an industrial robot arm that have been constructed make it possible to accomplish the task of selecting the optimum values of M_0 and b. We will assume that the allowable positioning error must not exceed the value Δ and that the robot's design makes it possible to alter the parameters M_0 and b within the bounds M_0 is a member of the set [0, M] and b is a

member of the set [0, b]. It is then possible to formulate the optimization problem in the following manner: from the entire set of values of the parameters M_0 is a member of the set [0, M] and b is a member of the set [0, b] at which the amplitude of the gripper's vibrations after the arm collides with the stop is less than Δ, determine those values of the parameters M_0 and b at which the time T required for the arm to turn is minimum. As an example, the specified problem is solved for the case b = 210 kg·m^2/s, M = 100 N·m, and $\varphi_0 = 5\pi/12$. The robot's design parameters corresponded to the example examined above. The amplitude of the gripper's vibrations after the arm collided with the stop and the time required for the arm to turn were determined for various values of M_0 and b. It turned out that the optimum parameters are as follows: for Δ = plus or minus 1.5 mm, $M_0 = 12.436$ N·m, b = 210 kg·m^2/s, and T = 4.457 s. For Δ = plus or minus 3 mm, $M_0 = 24.87$ N·m, b = 210 kg·m^2/s, and T = 2.246 s. For Δ = plus or minus 6 mm, $M_0 = 49.73$ N·m, b = 210 kg·m^2/s, and T = 1.14 s. For Δ = plus or minus 15 mm, $M_0 = 100$ N·m, b = 198.11 kg·m^2/s, and T = 0.562 s. For Δ = plus or minus 20 mm, $M_0 = 100$ N·m, b = 185.44 kg·m^2/s, and T = 0.543 s.

The mechanical models constructed may thus have various applications in robotics. The solutions obtained on the basis of such models are rather simple, and their error is low.

Bibliography

1. Yudin, V. I., "Analysis of Vibrations of Manipulator's Boom," PRIKLADNAYA MEKHANIKA, AN SSSR, Vol 16, No 10, 1980, pp 108-115.

2. Biderman, V. L., "Teoriya mekhanicheskikh kolebaniy" [Theory of Mechanical Vibrations], Moscow, Vysshaya shkola, 1980, 408 pages.

3. Polyakhov, N. N., Zegzhda, S. A., and Yushkov, M. P., "Teoreticheskaya mekhanika" [Theoretical Mechanics], Leningrad, Izd-vo LGU, 1985, 536 pages.

UDC 621.865.8

Required Precision of Stopping Moving Manipulation Robot Close to Workpiece

[Article by A. K. Kovalchuk, candidate of technical sciences and docent, V. I. Lobachev, candidate of technical sciences and docent, and V. V. Yarots, graduate student; first paragraph is IZVESTIYA VYSSHIKH UCHEBNYKH ZAVEDENIY: MASHINOSTROYENIYE abstract]

[Text] This article presents the results of experimental research permitting the well-founded specification of requirements for the precision of stopping a moving manipulation robot close to a workpiece.

Developing a control system to control the motion of a moving manipulation robot's carrier close to a workpiece requires data about the required control precision. Since there are no such data, additional research is necessary.

We will examine the process of controlling the motion of a moving manipulation robot in the stage in which it moves close to a workpiece (Figure 1). The control functions performed by the operator link the running coordinates of the mass center of the moving manipulation robot's carrier and the distance from it to the workpiece.[1] Let R_H be the vector of the generalized coordinates of the mass center of the moving manipulation robot's carrier in an inertial coordinate system and let R_0 be the vector of the generalized coordinates of the workpiece in the same coordinate system. It is then possible to write $(R_0 - R_H) = L$, where L is the generalized vector of the relative state of the mass center of the moving manipulation robot's carrier and the workpiece.

When solving problems of the proximity of a moving manipulation robot and workpiece, the precision of guiding the carrier is determined by the degree to which the specified boundary conditions at the point of the end of the maneuver at the time point t_k are satisfied. This precision characterizes the deviation vector $\Delta L(t_k) = L_i(t_k) - L_r(t_k)$, where $L_i(t_k)$ and $L_r(t_{kR})$ are the ideal and real values of the relative state vector.[2]
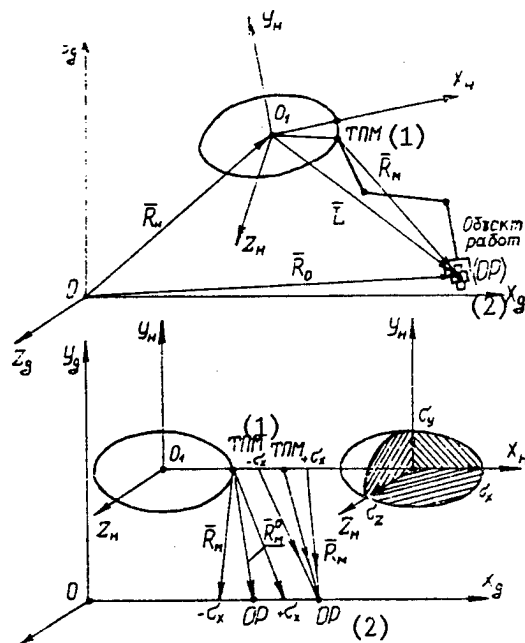

Figure 1. Process of Controlling the Motion of a Moving Manipulation Robot During the Stage in Which it Moves Close to a Workpiece

Key: 1. Point of the manipulator's suspension on the housing of the moving manipulation robot's carrier 2. Workpiece

The vector $\Delta L(t_k)$ may be represented in the form of the sum of the vector of the mathematical expectation and some centered random vector $\Delta L(t_k) = M\Delta L(t_k) + \Delta L^{(0)}(t_k)$.

The following correlation matrix may be taken as the characteristics of the precision of the approximation

$$K_L(t_k) = \begin{vmatrix} \sigma_x^2 & k_{12} & k_{13} \\ k_{21} & \sigma_y^2 & k_{23} \\ k_{31} & k_{32} & \sigma_z^2 \end{vmatrix}$$

where σ_x^2, σ_y^2, and σ_z^2 are the mean quadratic error of the respective component of the relative state vector and where K_{ij} (i, j = 1, 2, 3, with 1 being unequal to j) are the coefficients of the correlation between the errors of the components of the relative state vector.

The matrix $K_L(t_k)$ characterizes the region of the deviation of the components of the relative state vector $\Delta L(t_k)$ from the required values, i.e., the ellipsoid of dispersion is specified with regard to the relative coordinates.

We will assume that the guidance errors with respect to each coordinate are subject to a normal distribution law with the dispersion σ^2 and the mathematical expectation $[M] = 0$.[2] It is possible, with a precision that is tolerable for practice, to postulate that the errors in guiding a moving manipulation robot toward a workpiece with respect to each coordinate are mutually independent. The correlation matrix then assumes the following form: $K_L(t_k) = \text{diag} [\sigma_x^2, \sigma_y^2, \sigma_z^2]$.

The precision of guiding a moving manipulation robot's carrier to a workpiece may thus be determined if the values of the error dispersions relative to each coordinate are known.

To determine the dispersion of the errors in guiding a moving manipulation robot's carrier to a workpiece with respect to each coordinate, we will begin from the distinctive features of the working operations that must be performed: the kinematic parameters of the manipulator's end-effector and the method used by the operators to observe the performance of these working operations.

The mathematical expectation M[T] of the performance time when a slave manipulator is used to perform different working operations was determined as a result of the experimental studies conducted. A standard working operation with a medium degree of complexity was selected for further research.

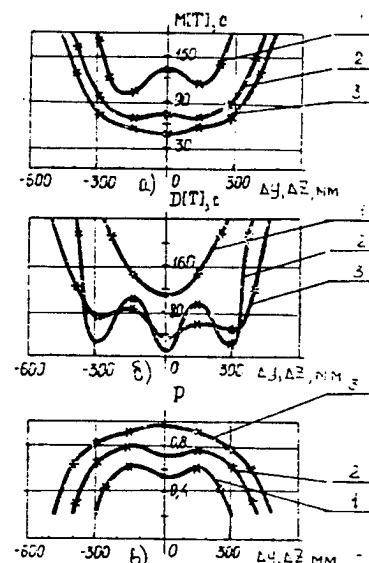The experimental research made it possible to establish dependencies between the mathematical expectation M[T] of the time, the dispersion D[T] of the time, and the probability P of the performance of the standard working operation and the shifting Δx, Δy, and Δz of
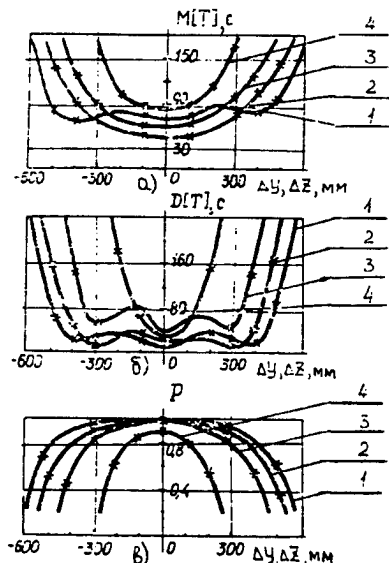
Figure 2. Dependencies Between the Mathematical Expectation M[T], Dispersion D[T], and Probability P of the Performance of the Standard Working Operation and the Shift x, y, and z of Assembly Components in the Manipulator's Work Zone in the Case Where an Operator Directly Observes the Course of the Working Operation; R_m, mm: 1, 600; 2, 700; 3, 800; and 4, 900.

Figure 3. Dependencies Between the Mathematical Expectation M[T] and Dispersion D[T] of the Time and the Probability P of the Performance of the Standard Working Operation and the Shift x, y, and z of Assembly Components in the Manipulator's Working Zone When the Operator Observes the Course of Working Operation (for R_m = 800 mm) by Using Mono (1) and Stereo (2) Television Units. (The Lines Labeled (3) Indicate Direct Observation.)

assembly components in the manipulator's work zone. In the case where the operator directly observes the course of the working operations, these dependencies have the form presented in Figure 2.

To estimate the effect of the observation method on the efficiency (i.e., on M[T] and P) of performing the standard working operation, analogous experiments were conducted with the operator using mono and stereo television units in his observation (Figure 3).

It is evident from the graphs that M[T] and the dispersion D[T] characterizing the convenience of the operator's work are very much dependent on the observation method.

In accordance with the previously described method,[3] the concept of the optimum working zone of the working operation is introduced as that part of the manipulator's

working volume in which the specified working operation may be performed with the required effectiveness. The location of the moving manipulation robot's carrier relative to the workpiece such that the workpiece is in the optimum working zone of the working operation is a requisite of the effective performance of the specified working operation by the moving manipulation robot's manipulator. The problem of determining the dispersions of the error in guiding the moving manipulation robot to the workpiece in the first approximation may then be viewed as a problem of determining the optimum working zone of the working operation, i.e., the linear dimensions Δx, Δy, and Δz of the optimum working zone may be viewed as the main axes σ_x^2, σ_y^2, σ_z^2 of the ellipsoid of the dispersion with respect to the relative coordinates (Figure 1b).

Table 1.

M[T], s	P	Observation Conditions	σ_x, m	σ_y, m	σ_z, m
60	1	direct observation	0.03	0.1	0.1
		observation by stereo TV	-	-	-
		observation by mono TV	-	-	-
	0.75	direct observation	0.05	0.2	0.2
		observation by stereo TV	-	-	-
		observation by mono TV	-	-	-
	0.5	direct observation	0.08	0.25	0.25
		observation by stereo TV	-	-	-
		observation by mono TV	-	-	-
100	1	direct observation	0.05	0.2	0.2
		observation by stereo TV	-	-	-
		observation by mono TV	-	-	-
	0.75	direct observation	0.1	0.3	0.3
		observation by stereo TV	0.08	0.2	0.2
		observation by mono TV	-	-	-
	0.5	direct observation	0.12	0.4	0.4
		observation by stereo TV	0.1	0.3	0.3
		observation by mono TV	0.03	0.1	0.1
140	1	direct observation	0.1	0.2	0.2
		observation by stereo TV	-	-	-
		observation by mono TV	-	-	-
	0.75	direct observation	0.13	0.35	0.35
		observation by stereo TV	0.1	0.3	0.3
		observation by mono TV	-	-	-
	0.5	direct observation	0.15	0.45	0.45
		observation by stereo TV	0.12	0.35	0.35
		observation by mono TV	0.05	0.1	0.1

A comparison of the dimensions of the optimum working zone of the working operation for different observation methods made it possible to establish the following relationships among them:

$$k_1 = v_1/v_0 = 0.7 \text{ to } 0.75;$$

$$k_2 = v_2/v_0 = 0.55 \text{ to } 0.65;$$

$$k_3 = v_3/v_0 = 0.2 \text{ to } 0.3;$$

where v_0 is the theoretical optimum working zone of the working operation, i.e., that volume in which it is theoretically possible for the manipulator's grip to move with the specified orientation (calculated for any mechanical diagram of the manipulator in accordance with the existing methods[4]), and v_1, v_2, and v_3 are the optimum working zone of the working operation during direct observation, observation via a stereo TV, and observation via a stereo TV, respectively. The values obtained for the coefficients k_1, k_2, and k_3 make it possible to determine the requirements for the precision of guiding the moving manipulation robot's to a workpiece on the first approach from the standpoints of the specified mechanical diagrams of the manipulators, the observation methods, and the characteristics of the workpiece.

The specified experiments by means of the values of σ_x, σ_y, and σ_z (Table 1) make it possible to conclude that the requirements regarding the precision of controlling a moving manipulation robot close to a workpiece are strict. The blank lines in the table mean that it was not possible for the moving manipulation robot to perform the working operation within the specified time T and with the specified probability P while the various observation methods were used. The data in the table may explain those problems that arise when controlling a moving manipulation robot close to a workpiece.[1]

Bibliography

1. Yastrebov, V. S., "Teleupravlyayemyye podvodnyye apparaty (s manipulatorami)" [Telecontrol of Underwater Devices (With Manipulators)], Leningrad, Sudostroyeniye, 1973, 199 pages.

2. Agadzhanov, P. A., Duleviich, V. Ye., and Korospelova, A. A., "Kosmicheskiye trayektorii izmereniya. Radiotekhnicheskiye metody izmereniy i matematicheskaya obrabotka dannykh" [Space Measurement Trajectories. Radio Engineering Measurement Methods and Mathematical Data Processing], Moscow, Sovetskoye radio, 1969, 504 pages.

3. Lobachev, V. I., Kovalchuk, A. K., and Gorelov, L. V., "Issledovaniye optimalnykh rabochikh zon montazhnykh operatsiy, vypolyayemykh kopiruyushchim manipulyatorom. Mezhvuzovskiy sbornik VZMI" [Investigation of Optimum Working Zones for Assembly Operations Performed by Slave Manipulator. Interinstitutional collection of VZMI], Moscow, 1978, pp 97-100.

4. Ushakov, V. I., "Quality Analysis of Manipulator's Service Zone," IZVESTIYA VUZOV. MASHINOSTROYENIYE., No 6, 1977, pp 133-136.

©"IZVESTIYA VUZOv. MASHINOSTROYENIYE", 1988

UDC 921.9:531.3

Dynamic System of Precision Machine Tool and Its Features

18610402c Moscow IZVESTIYA VYSSHIKH UCHEBNYKH ZAVEDENIY: MASHINOSTROYENIYE in Russian No 12, Dec 88 pp 122-126

[Article by G. S. Ivasyshin, candidate of technical sciences and docent; first three paragraphs are IZVESTIYA VYSSHIKH UCHEBNYKH ZAVEDENIY: MASHINOSTROYENIYE introduction]

[Text] In view of the effect of slowly occurring processes on the output parameters of machine tools and the fact that the complete deformability of an elastic system depends on elastic carryover, it has been deemed advisable to estimate the dynamics of a precision machine tool with an allowance for inelasticity processes.

The method of the experimental investigation of elastic carryover with preliminary displacement is presented.

Based on the experimental investigation of elastic carryover with preliminary displacement for the case of dry friction, a conclusion is drawn regarding the change in the transfer function of the dry friction process.

In view of the increase in the requirements for the quality and technical level of precision metal-cutting machine tools used to machine components with a high precision from the standpoint of dimensions and geometry, problems related to the dynamics of slow processes have become timely. The dynamics of slow processes is the direction in the science of machine reliability that studies those changes in machine subassemblies and components that occur over the course of protracted time intervals as a result of the effect of various energy sources on the machine.[1] Previous works[2-4] have concluded that, in view of the fact that the deformations of components in the elastic region during extension (compression), buckling, and torsion are accompanied by an elastic carryover and the output parameters of precision metal-cutting NC machine tools are commensurate with the deformations of the elastic carryover, it is necessary

to consider the effect of the imperfections in the elasticity of metals when designing precision technologies. The timeliness of a physical approach[1] to creating high-reliability machines and mechanisms stems from the fact that physical regularities lie at the basis of losses in efficiency.

Elastic carryover, i.e., time-delayed elastic deformation, is a reversible process that characterizes energy dissipation. In the general case, elastic carryover is the property of a material to turn the work of deformation back in time during unloading. It should be noted that a portion of elastic deformation does not disappear instantaneously but rather remains because of a specified quantity of potential energy (from 5 to 15 percent of the entire amount of energy expended on deformation). The effect of elastic carryover on the output coordinates of the elastic system of a precision metal-cutting machine tool increases as the use of plastics in machine building increases.

Elastic carryover constitutes 0.1 to 0.001 of the respective elastic deformations and is one of the imperfections of elasticity (i.e., inelasticity processes). Elastic carryover may cause errors in precision machine tools because of additional deformations in the machine tool component. It is therefore necessary, for example, to consider the elastic carryover of the material of a lead screw and nut of precision metal-cutting machine tools when making a transition to positioning involving fractions of microns and discreteness on the order of fractions of microns as well as when manufacturing components with a precision on the order of microns or fractions of microns.[2] Precision alloys with a regulated elastic carryover should be used when designing the spindle assemblies of precision machine tools.[4]

Based on the aforementioned, some ideas regarding the existing models for designing the dynamic system of a machine tool have changed.[5] The closed dynamic system of a metal-cutting machine tool is conditionally represented in the form of a block diagram whose individual blocks, (the elastic system and working processes, i.e., cutting and friction processes and the processes in the motor) are considered elements of the machine tool's dynamic system (Figure 1a). The following exert an effect on the elastic system: the impressed forces f(t), the cutting force P, the friction force F, and the moving force of the electric motor M. A reversible deformed effect $y(t)$, y_1, y_2, and y_3 corresponds to each force effect f(t), P, F, and M.

In view of the fact that elasticity processes must be considered[2] when creating precision metal-cutting machine tools, the closed dynamic system of a precision metal-cutting machine tool may be conditionally represented in the form of the block diagram shown in Figure 1b.
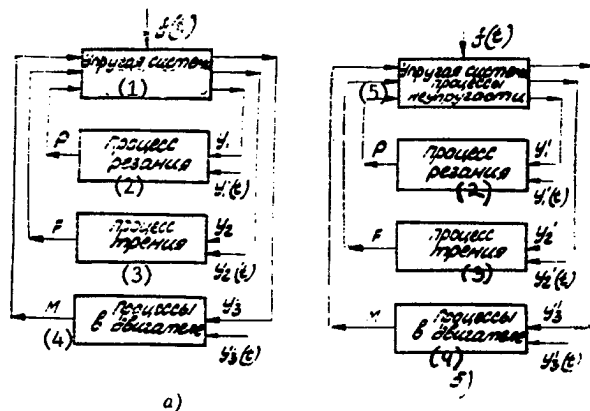
Figure 1. Block Diagram of the Dynamic System of a Metal-Cutting Machine Tool: a, Block Diagram According to V. A. Kudinov[5]; b, Block Diagram of a Precision Machine Tool.

Key: 1. Elastic system 2. Cutting process 3. Friction process 4. Processes in the motor 5. Elastic system; inelasticity processes

The input coordinates of the working processes of the dynamic system of a precision machine tool (Figure 1b) are described by the formulas:

$$y_1' = y_1 + \Delta y_1, \; y_1'(t) = y_1(t) + \Delta y_1(t),$$

$$y_2' = y_2 + \Delta y_2, \; y_2'(t) = y_2(t) + \Delta y_2(t), \; (1)$$

$$y_3' = y_3 + \Delta y_3, \; y_3'(t) = y_3(t) + \Delta y_3(t).$$

Under specified conditions, the imperfection of the elasticity (or inelasticity processes) exerts a great effect on the change in the elastic system's characteristics. The effect of inelasticity processes on the working processes, i.e., the cutting process, the friction process, and the processes in the motor, is in the form of additional deformation effects related to the phenomenon of elastic carryover. In this case, an additional reversible deformation effect $\Delta y(t)$, Δy_1, Δy_2, Δy_3 corresponds to each force effect $f(t)$, P, F, M.

Changing the properties of the material during the loading and unloading process, in particular, the Poisson coefficient, elasticity modulus, and shear modulus, as well as the constant relative microdisplacement of the solid bodies in space, largely depends on inelasticity processes. Additional displacements of components and unevenness in the movements of links and mechanisms occur under the effect of elastic carryover. The energy consumption required to set the links and mechanisms into motion is also corrected.

As an example, we will examine the effect of inelasticity processes, elastic carryover in particular, on the friction process in the form of additional deformation effects on the machine tool's elastic system. Elastic carryover constantly affects the conditions of the contact between

adjoining components of the machine tool.[6] The properties of the joint depend on the properties of the upper layers of the metal, which are responsible for the proximity of the components that are adjoined and the preliminary displacement. The rigidity of the surface layer affects the contact rigidity and strength.

Contact deformations (elastic and residual) in keyed and splined joints, on gear teeth, and in bearings increase angular displacements by 50 percent or more (according to data from Professor D. N. Reshetov).

It is known that the friction force is formed during the process of so-called preliminary displacement. The need to determine the factors affecting the significant instability of the preliminary displacement also makes it advisable to study the formation of preliminary displacement. In the work of P. M. Chernyanskiy,[7] for example, it is shown that even under unchanging conditions of the operation of one and the same design, the greatest and least displacements differ tens of times over. According to Z. M. Levina and D. N. Reshetov,[8] "the problem of the tangential compliance of joints is identical to the problem of preliminary displacement during friction."
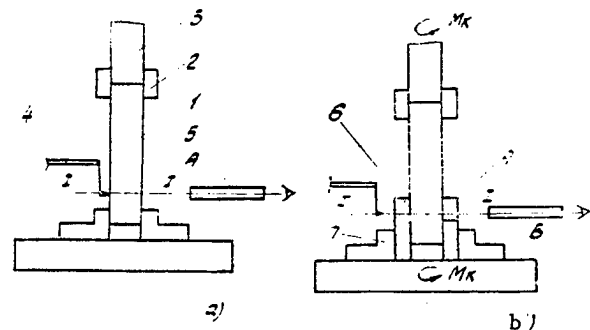

Figure 2. Diagram of the Configuration of the Measurement Terminal of a Variable-Induction Pickup and the Loading of a Specimen

Cylindrical specimens and a previously described[3] stand were used to study the preliminary displacement in joints. Figure 2 presents diagrams of the configuration of a measurement terminal and the loading of a specimen. A cylindrical specimen (1) from the grade of steel being tested is fastened in wedge grips (2) coaxially with the ram (3) of a single-vane hydraulic actuator (Figure 2a). Figure 3 shows two profilograms that have been recorded along the perimeter of the cross section of the specimen in position I-I of the terminal (4), which is connected with a model BV0844 variable-induction pickup. The profilograms are recorded with a model BV-862 recorder. The control profilogram (curve 1) in Figure 3 characterizes the profile of the specimen before loading. The profilogram (curve 1) is recorded according the previously described method.[3] A model AK-0.25 autocollimator was used to make parallel observations of the behavior of a fixed point A on the sample (Figure 2b).
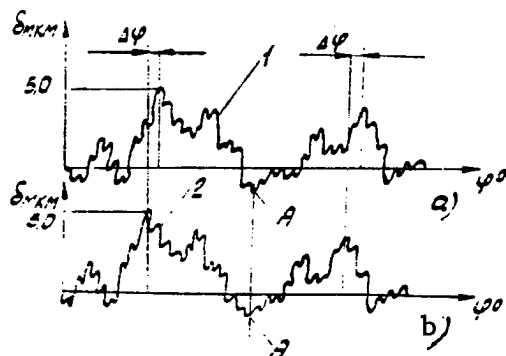
Figure 3. Profilograms: a, Control Profilogram (curve 1); b, Deformation Profilogram (curve 2); , Elastic Carryover During Preliminary Displacement.

After curve 1 is recorded, the lower end of the specimen is placed in a split bushing (6) that is then fastened in the chuck jaws (7) of the table (8) of a measuring machine. The centering of the specimen is maintained by observing the position of point A on the specimen through a special slit in the bushing through an autocollimator. A mode of preliminary displacement is created in the bushing-specimen pair by turning the measuring machine's indexing table or ram of the single-vane hydraulic actuator. The deformation profilogram (2) is recorded after the primary preliminary displacement and after the occurrence of elastic carryover in the surface layers of the components. The microturning of the measuring machine's indexing table ensures the occurrence of a preliminary displacement in the material of the contact that is solely dependent on contact preliminary displacement as a result of elastic carryover. It was established experimentally that, for 40Kh hardened steel, the contact preliminary displacement as a result of elastic carryover amounts to 0.2 to 0.3 μm. The time of the occurrence of elastic carryover in the material ranges from 10 to 15 minutes.

By providing preliminary displacement in the same bushing-specimen pair by using the single-vane hydraulic actuator to turn the specimen, it is possible to initiate a preliminary displacement in the contact material that depends both on the contact preliminary displacement as a result of the elastic carryover and on the preliminary displacement, which depends on the bulk preliminary displacement resulting from the elastic carryover. In this case, as experiments have shown, the contact preliminary displacement amounts to 2.0 to 3.0 μm, and the elastic carryover in the material of teh joint lasts from 15 to 20 minutes. Figure 3 the amount of the elastic carryover may be estimated on the basis of the angle φ_0 of the straightening of profilograms 1 and 2. Curve 2 interprets the elastic carryover during preliminary displacement. The unchanged position of point A on the specimen and on profilogram 2 is explained by the fact that, when the bushing turned, the surface of the specimen in the zone of point A was free from a load thanks to a groove in the bushing.

The input coordinate y_2' of the friction process changes under the effect of the elastic carryover of the elastic system

$$y_2' = y_2 + \Delta y_2, \text{ (2)}$$

where y_2 is the output coordinate of the elastic system, which depends on the elastic deformation, and Δy_2 is the output coordinate of the elastic system, which depends on the elastic carryover.

The static characteristic of the friction has the form

$$K_t = F/y_2' = F/(y_2 + \Delta y_2). \text{ (3)}$$

The time constant of the preliminary displacement and the slide velocity v = const

$$T_t' = l'_t/v, \text{ (4)}$$

where l'_t is that portion of the preliminary displacement that includes the elastic carryover during preliminary displacement. The existing formula[5] for the transfer function W_t of the dry friction process, which is based on equations for the deformation of a viscoelastic body, will have the form

$$W_t' = F/y_2' = K_t'/(T_t'p + 1). \text{ (5)}$$

The results obtained may be used in analyzing the characteristics of the friction process and in investigating and calculating preliminary displacement, positioning precision, and contact rigidity.

Conclusions

1. In view of the effect of slowly occurring processes on the output parameters of metal-cutting machine tools and the fact that the complete deformability of an elastic system depends on elastic carryover, it is possible (as a development of the theory of V. A. Kudinov) to estimate the dynamics of a precision machine tool with regard to inelasticity processes.

2. Because the friction force is formed in the preliminary displacement process, the elastic (reversible) portion of which depends on the elastic carryover, the effect of elastic carryover should be considered when estimating the output coordinates of the friction process. The size of the static characteristic of the friction depends on the elastic carryover.

Bibliography

1. Pronikov, A. S., "Nadezhnost mashin" [Reliability of Machines], Moscow, Mashinostroyeniye, 1978, 592 pages.

2. Ivasyshin, G. S., "Twisting of Lead Screws of Metal-Cutting Machine Tools," IZVESTIYA VUZOV. MASHINOSTROYENIYE, No 1, 1985, pp 131-135.

3. Ivasyshin, G. S., "Method of Investigating Poisson Coefficient During Process of Relaxation of Metals," IZVESTIYA VUZOV. MASHINOSTROYENIYE, No 4, 1983, pp 137-140.

4. Ivasyshin, G. S., "Effect of Elastic Carryover of Material of Spindles on Rocking Resistance in Spindle Supports," IZVESTIYA VUZOV. MASHINOSTROY-ENIYE, No 9, 1987, pp 125-130.

5. Kudinov, V. A., "Dinamika stankov" [Dynamics of Machine Tools], Moscow, Mashinostroyeniye, 1967, 360 pages.

6. Konyakhin, I. R., "Investigation of Deformation of Surface Layer During Contact Interaction," IZVESTIYA TOMSKOGO POLITEKH-NICHESKOGO INSTITUTA, Vol 68, No 1, 1951, pp 338-347.

7. Chernyanskiy, P. M., "Model of Tangential Displacements in Production System," IZVESTIYA VUZOV. MASHINOSTROYENIYE, No 10, 1984, pp 131-134.

8. Levina, Z. M., and Reshetov, D. N., "Kontaktnaya zhestkost mashin" [Contact Rigidity of Machines], Moscow, Mashinostroyeniye, 1971, 264 pages.

621.865.8.004.14;621.941.23-529;621.941.1.077

Using Robotic Lathe Complexes in Small-Series Production

[Article by M. I. Irodov, G. Ye. Sizova, A. F. Peretrukhin, and A. M. Kopeykin, engineers]

[Text] The Proletarian Freedom Plant is the head enterprise of the Yaroslavl Machine Building Production Association. In a 2-year period (1985 to 1987), eight lathe robotic production-process systems were introduced at the plant. The complexes, which were developed and manufactured by the Moscow machine building plant Red Proletarian, include model M10P 62.01 built-in industrial robots and a model M20P 62.01 floor-model robot.

Plans for retooling the plant call for converting the NC machine tool section on whose basis the robotic production-process system was introduced into a special shop where components for the entire association will be machined. The production is small-series production, with the average lot size not exceeding 30 to 40 components. Using a robotic production-process system here to machine body-of-revolution-type components (shafts, flanges, axes, disks, etc.) in an automated mode makes it possible to reach a fundamentally new level of organizing production by using the principles of group machining.

Definite experience in operating NC machine tools has already been accrued at the plant. The NC machine tools have been placed in a special section, services responsible for adjusting and repairing systems have been created, a special group of programmer-process engineers who work on preparing for the transition to machining components on NC machine tools has been created, and versions of material and morale incentives have been tried. A number of problems in the technological preparation of small-series production have been solved by specialists at the Yaroslavl Polytechnic Institute. The currently existing organizational structure for managing work to introduce robotic production-process systems has made it possible within the span of 1 ½ years to create a robotic production-process system minisection based on an NC machine tool section. This was preceded by work to introduce and operate an MK 6783 lathe complex (created on the basis of the existing model 16K20F3S5 NC machine tool and the separately acquired model SN 33 08.01 industrial robot), on which, like on a polygon, many problems of an organizational and technological nature were worked out.

The training and retraining of robotic production-process system operators and adjusters was based at the Gorkiy Institute of Increasing Qualifications and the Moscow machine building plant Red Proletarian.

In the stage in which a robotic production-process system is introduced it is necessary to overcome a number of subjective and objective obstacles. The main objective causes for these were design omissions by the manufacturing plant and the resultant low reliability of the equipment manufactured. The following turned out to be the most important design omissions. The workspace of the worker-operator was combined with that of the industrial robot (which does not ensure the working safety of service personnel). The overall dimensions of the cycle tables are unsatisfactory. Given the existing shortage of production areas, the tables' dimensions were cut in half (reduced to 12 positions). Six of the eight complexes lack systems for removing chips from the trays. The driver chuck was not shipped as a complete unit, which makes it impossible to machine shafts on model 16K20F3R132 chucking-center robotic production-process system. The positioning of a configuration of components is insufficiently precise, which increases defective production. When components with class 8 precision are machined, they are generally mounted manually. It should also be noted that there is a problem in acquiring component products, particularly the 21MVN electric motor (produced in Bulgaria).

The second group of problems was directly related to the organization of the production process.

Precisely guaranteeing the rhythmic operation of the robotic production-process system plays no small role. This is the responsibility of the plant's planning and dispatch service. The problem of loading a robotic production-process system under conditions of small-series production should be solved by consolidating component lots, i.e., by creating groups of single types of components based on standardization and unification. As the experience of operating robotic production-process systems has shown, a component lot size of no fewer than 50 units should be considered optimum since smaller component lots require a great deal of time to retool the complex, which reduces the effect of using the complex substantially.

The problem of consolidating component lots at the plant is slated to be solved by machining body-of-revolution-type components for the entire association in a section equipped with a robotic production-process system.

This requires precise planning based on a multiversion calculation that makes it possible to react quickly to changes in the production process. A computer center that is used in solving these problems has been created at the plant.

The operation of the blanking section still remains an unsolved problem. Blanks arriving for automated machining do not meet size stability requirements, which frequently results in the breakdown of the cutting tool and in defective production. As a result, the components that are being sent to the robotic production-process system must be subjected to preliminary roughing. The experience of a number of the oblast's machine building enterprises confirms the wisdom of this approach.

Some of the forces involving the human factor are worth noting. Specifically, the interests of specialists from the plant's various services in solving problems related to introduction and operation must be combined. Work must be assessed on the basis of the end result. Consideration must be given to the disinterest of process engineers involved in developing the production process entailed in manufacturing components in the end result—in the introduction of new technologies for robotic production-process systems (i.e., for the lack of "author's" control on their part) and to the machine tool operators' lack of desire to service new technology on account of the frequent soft failures of individual elements in the system, defective components with a low positioning precision, and a lack of material interest. Solving these problems depends on labor organization that conforms with the level of the technology being used.

The brigade form of labor organization was tried in the section. Unfortunately, it was not developed owing to a number of objective factors. The robotic production-process system's operators and adjusters currently work individually. The section operates on two shifts. Two operators and two adjusters work per shift (one operator for three robotic production-process systems and one adjuster for four or five equipment units).

Ways are now being sought to combine the functions of operators and adjusters and work in a single detail. it should be noted that the search for a form of organization is being conducted directly in the section and is not regulated by the plant's administration. It is planned that, as labor wages are improved, process engineers, repairers, and planners will be included in this brigade, i.e., a start-to-finish brigade that is interested in the end result will be created.

Introduction of the new production cycle under existing production conditions and under the existing organization has not been efficient and has created many problems. The need to use robotic production-process systems at all is, however, clearly recognized at all management levels.

By summarizing the results of the first year of the robotic production-process system's operation, it may be possible to identify those problems whose solution is critical to the successful introduction of robotics under the conditions of the existing production process: design decisions that have not been fully worked out must be refined on site; the frequent equipment failures that result in a significant productivity loss must be eliminated; the stability of blanks' parameters must be increased; working conditions must be improved; the entire organization of labor must approach the requirements of robotization; problems related with norming, material and morale incentives, and rewarding workers in consideration of their increased work responsibilities in automated production must be solved; and brigades consisting of workers and scientific-technical personnel must be created.

It should also be noted that a robotic production-process system disciplines production—this makes it necessary to plan shops, supply components in a rhythmic manner, use a special tray, etc. Robotic production-process systems must be maintained in accordance with the graph that has been developed, and they require constant author's supervision on the part of adjusters, process engineers, programmers, and repairers. Robotizing production requires developing tool shops and other plant services. An enterprise is not equipped to introduce dozens of robotic production-process systems at once. It must begin with a lesser number. Nevertheless, the step must inevitably be taken. Expenditures on technical organizational measures are justified during integrated robotization. Introducing a robotic production-process system requires raising the qualifications of service personnel, i.e., the preparation of personnel and a base for the maintenance of robotic production-process systems are required.

The main purpose of production is not to introduce individual robotic production-process systems but to develop the enterprise to the level required by new technology, organize the servicing of the new technology, and strengthen labor discipline and personnel training, i.e., to create a fundamentally new form of production organization that meets modern requirements.

©Izdatelstvo "Mashinostroyeniye", Mashinostroitel, 1989

621.838.5

Device for Machine Pneumonic

18610396b Moscow MASHINOSTROITEL in Russian No 2, Feb 89 pp 15-16

[Article by A. I. Korolkova, engineer]

[Text] The device (author's certificate 1315963) is intended to make machines pneumonic. It contains any number of power cylinders. Some of them are turned on several times per cycle, with the number of actuations differing in different cylinders.

The device changes the positions of the power cylinder's rod not only at the end of its course but also in any intermediate position in accordance with the position required of the machine assembly. It has pneumatic limit switches (T1 and T2) and a rack (Figure 1) located on a fixed base and a switch (B) mounted on the power cylinder's rod (11). The limit switches (T1 and T2) (in accordance with the number of cams) are each connected with the respective cam (3) of the switch (B).

Freely mounted on a fixed axis (5) in the case (2) of the switch (B) are a disk-shaped lever (6) with teeth (13) on the bottom and supporting dog (8) and a bushing (4). A

12-tooth ratchet wheel and change cams (3) representing a ring-shaped boss with two, three, four, or six teeth-lobes (Figure 2) are mounted on the bushing (4).
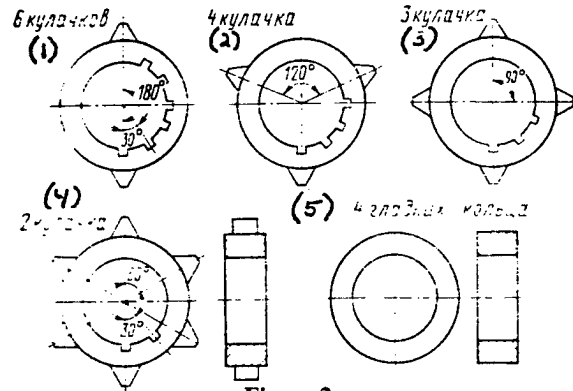
Figure 2

Key: 1. Six cams 2. Four cams 3. Three cams 4. Two cams 5. Four smooth rings

The number of change cams corresponds to the number of times the cylinder is switched on during the machine's operating cycle. The dogs (8) and (10) are pressed to the ratchet wheel by a spring, and the lever (6) is pressed to a pin (9).

Levers (15) (based on the number of change cams) sit on the case axis (14), with one lever under each cam. Each lever has a tooth (12) at the end. A spring-loaded follower (1) acts on the left arm of the lever and presses the end of the right arm to its cam. In the limit switches (T1 and T2 [shown in the cross section]) the casing (17) has a vertical slot in which a lever (21) freely sits on an axis (18). This lever (21) is fastened to a wider L-shaped plate. A spring (20) presses the switches to the case. A
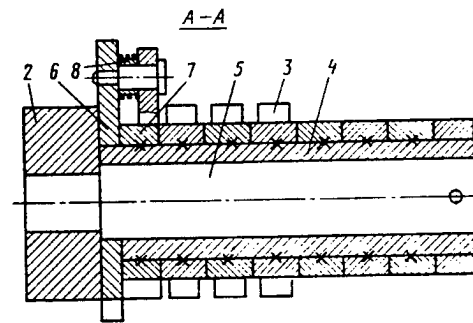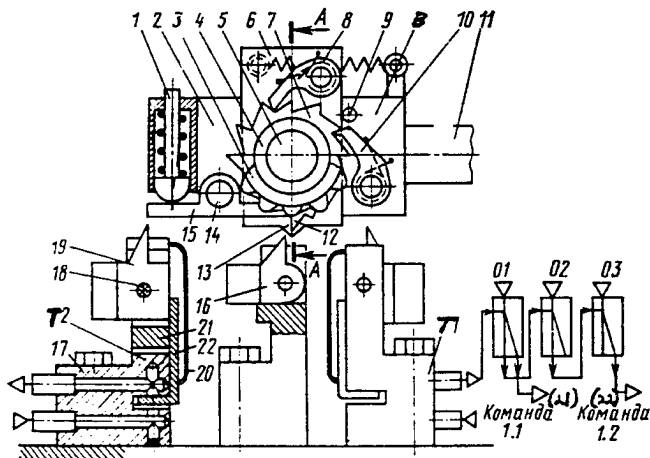

Figure 1

Key: 21. Instruction 1.1 22. Instruction 1.2

lever (19) with a thickened back, which is pressed by its own weight to the L-shaped plate, sits freely in the very same axis in the slot of lever (21). The horizontal flange of the plate enters the slot in the case and blocks the feed of compressed air into the fitting that issues the control instruction.

The rack is mounted on a fixed base. A hinged lever (16) that returns to its initial position under a load is located in the rack's slot on an axis.

When the switch (B) is moved to the left, the tooth (13) comes into contact with the hinged lever (16) of the rack, and in order to pass above it, it turns lever (6) with the dog (8), the ratchet wheel, and the bushing with the cams set in it counterclockwise. The tooth (13) and lever (16) are located such that the system turns at an angle that is barely larger than the spacing of the ratchet wheel. The tooth (13) bypasses the lever (16), which returns to its initial position up to a stop (9). However, the ratchet wheel and bushing with the cams remain turned at the angular pitch (30°). The spring-loaded dog (10) enters the ratchet wheel's space and locks it together with the bushing in the new position. At the next change cam, one of the lobes occupies the lower position and forces out the right arm of the lever (15) with the tooth (12).

When the switch (B) moves further to the left, the tooth that is lowered (12) turns the hinged lever (19) together with the lever (21) and the plate (22) counterclockwise, thus allowing the passage of a stream of compressed air through the communicating channels. The limit switch T2 sends a short pneumatic instruction pulse, and the rod assumes the programmed position, after which it moves to the right. Levers (19) and (21) return to their initial position.

At the end of its course to the right, tooth (12) acts on the limit switch (T1), which issues a control instruction.

When the power cylinder is turned on again, the switch (B) is activated again, the tooth of the second cam assumes the lower position, and the onswitching of the limit switches (T1 and T1) is repeated, only this time the limit switches are mounted at the beginning and end of the path under the second cam. These switches issue control instructions independent of the control instructions of the switches located on the first path, etc.

With K actuations of the power cylinder, the limit switches (T1 and T2) mounted on K paths under K ring cams issue independent, unrepeated control instructions in the cycle 2K. The same thing happens with the other cylinders, which are turned on several times during the machine's operating cycle. When all of the independent control instructions are communicated to the air distributors in accordance with the machine's operating cycle, the latter begins to operate in the automatic cycle programmed.

Despite the complexity of the problem being solved, the scheme for making a machine pneumonic is simple and comprehensible to service personnel.

The device makes it possible to implement K different positionings of machine assemblies with each of K linear movements or K turns of these assemblies by using cylinders that are actuated K times per cycle. This type of positioning may be required to operate machine tools, robots, etc.

A control instruction doubler (as is shown for T1) consisting of three logic elements 01, 02, and 03 should be attached to the outgoing connection of each limit switch. One of the control instructions, 1.1 for example, is fed to a high-pressure amplifier attached to the face of the distributor that must be switched at the completion of the positioning, whereas instruction 1.2 is fed to turn off the amplifier of the distributor that activated the rod's movement to the side of this switch. After this amplifier is turned off, the springs that are attached to the distributor's faces bring it to the middle position and lock the cylinder's piston and rod in the required position together with the machine subassembly being moved.

©Izdatelstvo "Mashinostroyeniye", Mashinostroitel, 1989

621.86.062;621.865.14

Gripping Devices

[Article by V. L. Kaner, engineer]

[Text] The All-Union Electrical Engineering Technology Planning and Design Institute [VPTIelektro] has developed a number of designs for gripping devices with expanded technological capabilities and increased operating reliability.

The fork grip (author's certificate 893847) ensures reliability during the operation of a loader with cargo whose mass ranges from 5 to 10 tons. The grip has forks (1) (Figure 1) mounted on a lifting carriage (5) by means of levers (3) and (4) with differing lengths. The levers are connected with the carriage and forks by hinges. The movement of lever (4) is restricted by stops (6).

In the initial position, the weight of the forks and lever is balanced by a spring (2), with the cargo surface of the forks being located horizontally. When the forks are loaded, the cargo surface turns, and the cargo ends up in a position that is convenient for transport. After the cargo is released by a spring, the cargo surface returns to the initial position.
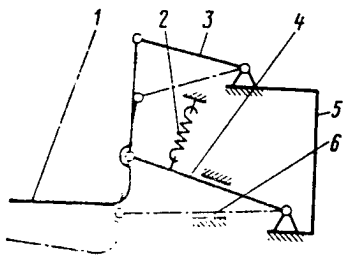
Figure 1

The vacuum grip for transporting sheet blanks (author's certificate 994243) contains a case (1) (Figure 2) with a cavity. A sealing ring (2) that is made of an elastic material and that extends beyond the working face of the case presses the gripper to the blank, thereby ensuring a leaktight connection and high operating reliability.
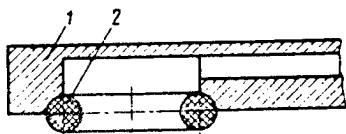

Figure 2

The electromagnetic grip (author's certificate 1199372) was developed to eliminate the simultaneous gripping of two or more blanks, which, when they are fed into a a die, results in increased wear to the die and its breakdown. A coil (5) (Figure 3) with a winding is mounted on a magnetic circuit (1). The central and upper portions of the magnetic circuit are threaded openings with bushings (3) and (6) twisted into them. The bushings contain magnetically controlled reed relay elements (2) and (4).
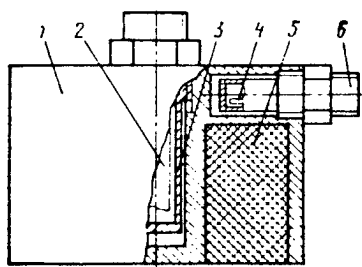
Figure 3

The bushings (3) and (6) are regulated to place the reed relays at the level at which the magnetic field (its force lines through the air gap are closed along the outer and inner walls of the magnetic circuit) is insufficient to activate them. The reed relays are only activated upon the closure of the magnetic flux through the material of blank (which has a low magnetic resistance), with reed relay (2) being activated when two or more blanks are gripped and reed relay (4) being activated when only one blank is gripped. The robot control system thus receives

precise information about the number of blanks being held by the gripping device.

A vacuum grip (author's certificate 1058865) that is based on an arm (8) (Figure 4), cross-piece (4), and suction cups (3) has been developed to ensure the reliable and precise gripping of only one flexible plate.
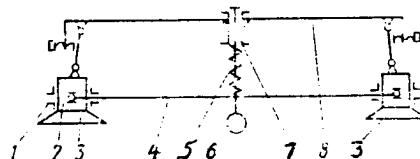

Figure 4

During its operation, the grip is lowered onto a stack of plates. First, a stop (6) makes contact with the stack. Moving along the cross-piece (4) with a rod (7), the stop compresses a spring (5) and raises the barrels (1).

When the grip is lifted, the cases (2) with the suction cups move along the inner surfaces of the barrels. A vacuum is formed under the suction cups. As a result the plate is lifted, bending relative to the stop (6). At the same time, the cases and barrels turn around, fastening themselves to the bent surface of the plate. The deformed plat is separated from the stack and transferred to the production equipment. The plate is separated from the grip when the air access in the suction cups is opened.

Figure 5 shows a vacuum grip (author's certificate 1281497) that differs from the one just described by the fact that its cross-piece (6) is in the form of a predeformed leaf spring and is mounted such that its concave side is turned toward the arm (5). When the grip is lowered, the top plate in the stack first touches the stop (8). Next, the cross-piece is straightened, and the rod (9) moves along the guide (7). The slide bars (1) turn from the center of the grip, and the springs (4) hold the case (3) with the suction cups in the extreme positions.
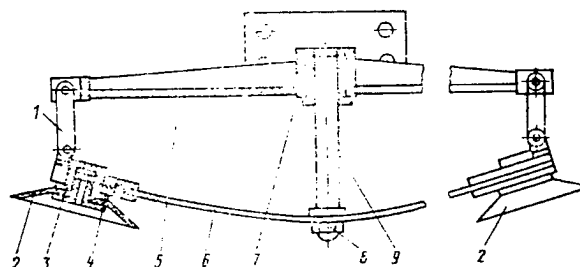

Figure 5

When the grip is raised, the stop (8) initially remains on the stack of components due to the effect of the elasticity of the cross-piece but the case (3) is raised and moves

along the slots, compressing the springs (4). A vacuum is created in the suction cups, and they pull the edges of the upper plate from the lower-lying one and bend it relative to the stop (8). Since the bending of the plate being raised and the leaf spring of the cross-piece corresponds to one and the same equation for a flexible line and since the suction cups are always perpendicular to the surfaces of the plates being raised, the grip's operating reliability is increased. Plates are separated from the grip when access to atmospheric air is opened in the suction cups, after which the springs (4) return to their initial position.

An electromagnetic grip (author's certificate 1299926) was developed to increase the reliability of activating a device to monitor for the presence in the grip of a component that has gotten hung up during transport. Electromagnets (2) (Figure 6) are mounted to the base (1). A case (5) with an electromagnet mounted in it is mounted in the center of the base on a guide bushing (4). It is capable of moving freely in the amount of the deviation of the component's (3) surface. A device (6) to monitor for the presence of a component in the grip is mounted on the case.
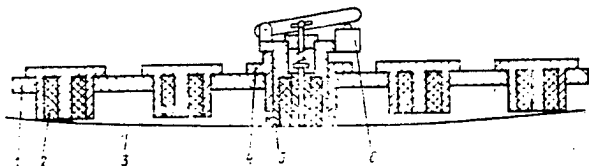

Figure 6

In its initial position, the case (5) is located in the lowermost position. When voltage is fed to the electromagnets' coils, the top component in the stack is pulled to electromagnets' faces. When the grip is raised, the component hangs for a while, as a result of which the case (5) moves, the control device (6) is activated, and a signal indicating the presence of a component in the grip is fed into the control system.

A gripping device (author's certificate 1283092) makes it possible to obtain required clamping force values at specified dimensions of components being gripped. Regulation of the device both increases the reliability of a grip for heavy components and eliminates damage to thin-walled components during clamping. The spread required of the device's jaws is minimal, which reduces power consumption.

When the device (Figure 7) operates, its screw (the drive is not shown in the figure) begins to turn. The sliding nuts, (6) and (1) and (5) and (2), move apart along the screw axis, forcing the parallelogram (4) with the jaws (3) holding the component to synchronously move together perpendicular to the screw. The components are released when the screw rotates in the opposite direction. To

regulate the parting of the jaws when making adjustments to machine a specified batch of components, a central gear that is connected to the sliding nuts by gears is set into rotation. As a result, these nuts rotate in different directions and move to one side, thereby making the jaws either come together or move apart through levers and hinges. To regulate the force with which a component is clamped, the screw (7) is turned, thus changing the angle between the levers that connect the sliding nuts and the parallelogram (the force is dependent on this angle). The amount of space between the jaws also changes. To keep this size fixed, the drive regulating their parting is turned on (not shown in the figure).
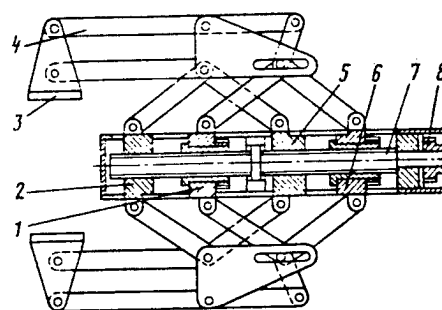

Figure 7

The magnetic-vacuum grip (author's certificate 1366396) for ferromagnetic and nonferromagnetic materials has an electromagnet (14) (Figure 8) that is located in a case (13) and a vacuum chamber that consists of a case (12) with rubber suctions cups (10) mounted in it. A diaphragm (11) that hermetically seals the joint of the touching surfaces of the cases (12) and (13) is attached to the case (13) and suction cup. Case (13) is placed in a barrel (7) that is hinged to the load-bearing device and can, together with the barrel, move vertically relative to case (12). Two arm levers (9) and springs (1) are provided for this purpose. The case (13) contains a sensor that issues signals regarding the magnetic properties of the material of the component that is being gripped and that contains a permanent magnet (15) mounted on a spring-loaded rod (6). The latter interacts with the sensor (5). In the interconnected channels of the case (13), there is a connecting piece (3) and spring-loaded valve (2) in one channel and a sensor (4) to monitor the reliability of the gripping of the component by the vacuum suction cup in the other. A potentiometer (8) is mounted in the barrel. The potentiometer's axis interacts with that of one of the two-arm levers (9).

Another gripping device (author's certificate 1425084) has clamping elements with heaters. Its casing (1) (Figure 9) is a plate with a flange for attachment to a transfer device. Arms (4) with clamping elements whose movement can be regulated are mounted in the slots of the
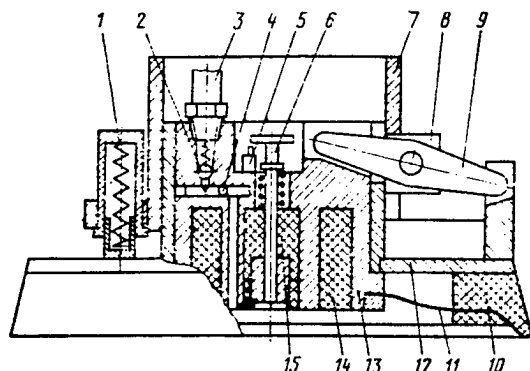
Figure 8

casing. The clamping elements are in the form of fingers (3) (made of a material with the property of shape memory) with jaws (2) on one end and heaters on the other.
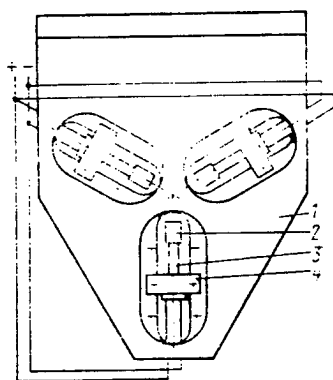

Figure 9

When a component is gripped, the heaters are turned on. They heat the fingers to the specified temperature at which the fingers "remember" the shape attached to them during the heat treatment, and they grip the component in their jaws. After the components move from the gripping zone to the unloading zone, the heaters are turned off and the fingers are cooled. When they reach a specified temperature they reassume their original shape, releasing the component from the jaws' grip.

The design simplicity of the gripping device and the absence of lever systems increases its reliability. Thanks to its compactness, the device can find wide use during the operation of production equipment under cramped conditions. The device is easy to readjust for different component type sizes by a readjustment in the arms (4).

Various modifications of the gripping device make it possible to clamp components both by the inner and outer surface or by both surfaces simultaneously or alternately. They also make it possible to transfer components with a complex shaped profile that lie not only vertically on a rib but also horizontally in a stack.

©Izdatelstvo "Mashinostroyeniye", Mashinostroitel, 1989

UDC 621.941.23-529;621.865.8.004.14;621.941.1.077

Robotic Production Module

18610396d Moscow MASHINOSTROITEL in Russian No 2, Feb 89 p 18

[Article by Ya. F. Vernigora, engineer]

[Text] The Kharkov Machine Building Design and Planning Technology Institute has developed and introduced a robotic production module with an automatic control system based on a model ATPr-2M12-SN1 machine tool and a model Brig-10 floor-model industrial robot (8) to perform 39 component-machining operations on each of 23 complexly shaped body-of-revolution-type components (flanges, valve bodies, valves, pinion blanks, etc.) with diameters ranging from 24 to 100 mm, lengths from 14 to 97 mm, and a mass of up to 5 kg.

The storage device (the gravity chute (6) of the robotic production module) is equipped with a set of changeable inserts (7) and locating rests (5) that orient any blank relative to the robot's gripping device (3) and, consequently, the base plane of the chuck's (2) jaws. The device accommodates from 13 to 50 blanks depending on their dimensions. It may be moved in a vertical plane and subsequently fixed.

A nozzle (4) to blow chips off the chuck jaws is mounted on the robot's ram. Air for the blowing is fed from the robot's pneumatic system in accordance with a program.

Adjusting the storage device for an operation entails fixing the blank's oriented position relative to the jaws' base plane by using the industrial robot, and adjusting the robot itself entails changing the gripping device's jaws for the respective range of blank diameters. The total time required for the adjustment is no more than 10 percent of the time required to adjust a machine tool for a production operation.

Two stand-alone robotic production modules performing one and the same task are located in a robotic robotized section. Their protracted operation has demonstrated their high reliability in performing complex lathing operations with an acknowledged design simplicity.
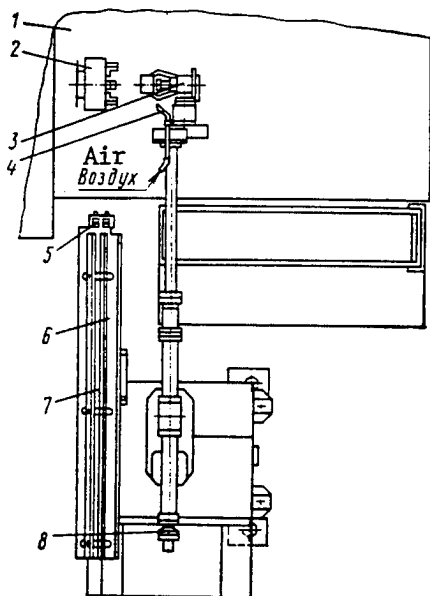
Robotic sections consisting of several stand-alone modules based on NC machine tools have a number of important advantages over sections where robot modules are linked to a continuous production process and constitute a robotic line. In the latter case, an insignificant failure or the shutdown of one of the line's components makes it necessary to shut down all of the production equipment to eliminate the failure. A section based on several stand-alone quick-change robotic production modules makes it possible to remove the failed module for repair, readjust the other modules quickly, and continue the production process. This makes it possible to increase the equipment's loading factor and to guarantee that a section will fulfill its production quota to a known degree.

UDC 621.9.06-529.003.13;658.512.011.56

Increasing Efficiency of Using NC Machine Tools

[Article by O. A. Novikov, B. Kh. Salatov, candidates of technical sciences, and A. Ya. Tyantov, engineer]

[Text] The efficiency of using NC machine tools as compared with other types of equipment should reduce machining costs. These costs consist of a number of components, the main ones being the following: costs related to controlling the machining process (i.e., toprepare the control program) and direct machining costs

(including deductions for equipment costs). The latter is greatly dependent on the duration of the cycle for machining each component. The cost of NC equipment is significantly greater than that of many other types of equipment, particularly universal machine tools with manual control. For this reason, using NC equipment efficiently requires, as a minimum, that the machining time be reduced in proportion to the increase in amortization deductions for the equipment's cost. But this does not occur in many cases, particularly under conditions of single-unit and small-series multiple-product production.

One way of increasing the efficiency of using NC machine tools under conditions of single-unit and small-series production is to use the machining techniques used in mass production, i.e., to use combined tools and multitool units, i.e., to use the principle of combining transfers in time. This approach is covered in the fundamental principles of modular technology.

The time required to machine components on NC machine tools may be reduced by creating the optimum sequence of working and auxiliary motions for the machine tool's actuators during the stage in which the control program is developed.

Each working machining cycle contains the time t_p required for a working pass by an actuator and the time t_B required for noncombined auxiliary passes:

$$T_{\text{u}} = \sum_{i=1}^{n} t_{p_i} + \sum_{j=1}^{m} t_{B_j}.$$

In one working pass it is possible to machine only one surface or else machine several surfaces in parallel by a multitool unit or a combined tool. In the latter case, t_p is specified as the time interval between the moment at which the tool makes its first cut and the time when it leaves the cutting zone. The process of machining on a machine tool may be represented as some transformation of a production object from the initial state C_H to the end state C_K.

This sequence corresponds to some sequence of alternating working and auxiliary passes of the machine tool's actuators over time:

$$\boldsymbol{P}: [t_{B_1}] \rightarrow t_{p_1} \rightarrow [t_{B_2}] \rightarrow t_{p_2} \rightarrow \dots$$
$$\dots \rightarrow [t_{B_{m-1}}] \rightarrow t_{p_n} \rightarrow [t_{B_m}].$$

The brackets indicate that different auxiliary motions are not mandatory during the transition from one working pass to another.

In this case, for the established set of working passes (which are determined by the content of the operation), it is possible to to reduce the time of the machining cycle T_c by developing a sequence of operations at which the sum

$$\left(\sum_{j=1}^{m} t_{B_m} \right)$$

of the auxiliary time during the transition from one working pass to another is the minimum. Assuming that the number of working passes in an operation equals n, we obtain all possible versions of their sequence as the number of transpositions P_n. This may be illustrated by using the graph shown in Figure 1. Its nodal points are the time required to implement the first through n-th working passes. The graph's nodes are the initial (C_H) and end (C_K) states of the production object. The information regarding the graph's branches is as follows: t_B is the time required for the auxiliary passes that are needed to progress from the j-th working pass to the (j + 1)-th.
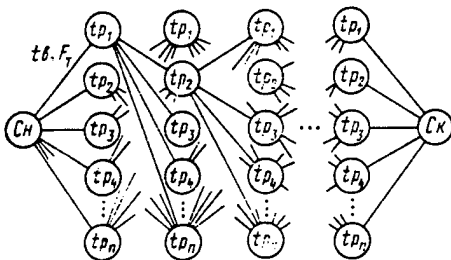

Figure 1

Some reasons why a working pass cannot be implemented are as follows: the adjustment base for implementing a working pass entailed in machining a surface may be lacking, one surface may be covered by an allowance layer belonging to another surface, etc. In these cases, the version of the working pass sequence is excluded from examination.

The entire task is thus reduced to searching for the shortest (from the standpoint of time) route on the graph. Algorithms for solving such problems have been rather well developed.[1] In the case where the content of an operation is distinctly divided into stages (roughing, semifinishing, finishing) it is possible to solve this problem in a step-by-step manner after representing the operation in terms of a number of transformations ($C_{H\ i}$ to $C_{K\ i}$), i = 1, ..., m.

The proposed method of increasing the efficiency of the functioning of NC machine tools makes it possible to estimate the efficiency of using multitool units as compared with single-tool machining. In this case the operation graph will be unloaded. When switching to a higher lever of CAD for the technological preparation of production it is possible to compare the effect achieved by using multitool units with the time expenditures required to adjust the graph, i.e., it is possible to proceed to an analysis of the operation's cost.

Footnotes

1. Yevstigneyev, V. A., "Primeneniye teorii grafov v programmirovanii" [Using Graph Theory in Programming], Moscow, Nauka, 1985, 352 pages.

Pallet for Flexible Manufacturing System

[Article by S. V. Maslov, engineer]

[Text] One way of reducing unproductive expenditures under conditions of automated production is to reduce different types of transport and mounting transfers of blanks within the confines of a shop, section, or machine tool work area.

In flexible manufacturing systems for machining bodies of revolution, the traditional configuration called for transferring honeycomb-type containers (pallets) between machine tools in accordance with the production route along with robots that transfer blanks from the containers to the machine tool's clamping attachments for machining and then back to the containers after the machining has been completed.

To eliminate extra expenditures of auxiliary time on such operations as drilling, milling, and threading that are performed from the face side of the components undergoing preliminary lathing it is possible to use a satellite-pallet, which makes it possible to base and mount a blank directly in its case.

The prisms (7) (Figure 1) in which the blanks (2) are based are attached to the frame (1) of the satellite-pallet by screws. They are then fixed with the help of tightening devices by strips (4). The satellite-pallet's entire mechanism is covered with covers (3). The even envelopement of all the blanks along the arc guarantees an identical clamping force, and using a steel strip as a clamping element makes it possible (in view of the rather large contact area) to reduce the pressure on the blank and to thus avoid any possible deformations of the blank. Rollers (6) ensure the waveform shape of the strip when no blanks are present.
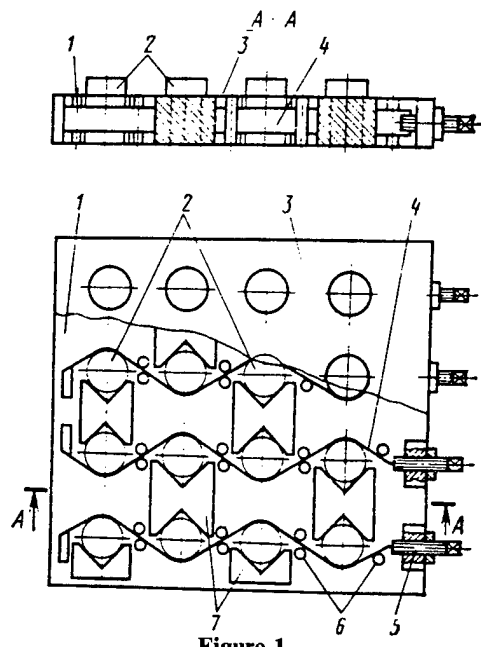
Figure 1

A robot (for example, an Elektronika NTs TM-01) servicing the lathe loads blanks into the satellite-pallet. The blanks may be fixed in the satellite-pallet on a stand equipped with an electromechanical power nut driver. Devices equipped with relay automation equipment are sufficient to configure the satellite-pallet on and remove it from the machine tool.

©Izdatelstvo "Mashinostroyeniye", Mashinostroitel, 1989

UDC 621.9.06-229.3;621.941.28-229.3

Equipment for Mechanizing Vertical Boring and Turning Machines

18610396g Moscow MASHINOSTROITEL in Russian No 2, Feb 89 p 20

[Article by A. V. Pronchenko, N. G. Gutnik, and L. M. Filimonova, engineers]

[Text] The heavy machine building sector maintains a large park of large vertical boring and turning machines whose mechanical face-chuck jaws are set into motion by a machine tool operator by using a screw or wrench with an extension piece or a wrench with a truncated arm that is adapted for the blows of a sledge hammer. This heavy manual labor is very traumatic and entails increased wear to the jaw screws.

The blanks that are machined on large vertical boring and turning machines are generally large-mass castings and forgings without high-quality base surfaces. Consequently, the alignment process, i.e., matching the blank's rotation axis with that of the chuckplate in horizontal and vertical directions, is very difficult. In practice, wedges and sledge hammers are used to do this, and the shop's crane equipment is diverted for a long time.

Work is underway at the Kramatorsk Machine Building Design, Planning, and Technology Scientific Research Institute to mechanize the alignment and mounting of large blanks on heavy vertical boring and turning machines. The ordinary jaw in the jaw housings is thus replaced by a mechanohydraulic one. It may be used to mount components with significant forces when a moderate torque is applied as well as to align a blank in a horizontal direction.

The mechanohydraulic jaw (Figure 1) consists of a housing (1) and large (3) and small (5) pistons. The latter is mounted on thrust bearings and is actuated by a screw (4). The jaw is brought into contact with the blank by the screw in the jaw, after which a mechanohydraulic mechanism that is built into the jaw is used. The rotation of the screw (4) sets the small piston in motion. It forces oil out of the large piston's compartment and into the compartment of the housing, thus forcing the large piston to move. The force created is monitored by a pressure gauge that is calibrated in tons force. For safety's sake, after the component is fastened, the large piston is braced by a threaded stopper (2), which keeps the blank from becoming unfastened in the event of an unforeseen oil leak. The estimated force on the large piston from an applied torque of 190 N·m amounts to 350 kN (35 tons force). In one turn of the screw the large piston moves 0.4 mm.

A mechanohydraulic jack with a lifting capacity between 80 and 100 tons (Figure 2) has been developed for vertical alignment. Its operating principle is the same as that of the mechanohydraulic jaw. To make working the jack convenient and to give it smaller overall dimensions, the small cylinder is divided into two parts and is manufactured from two pipes (3). The rod of the large piston ends in a floating thrust journal (1). A pressure gauge (2) that is also calibrated in tons is provided to monitor the force created. In one turn of the screw the jack raises its load 0.2 m.

A lighter-weight jack with a lifting capacity of 50 tons has also been developed.

A standardized ratchet wrench with special adapters has been created for convenience in working with the jaw and jack.
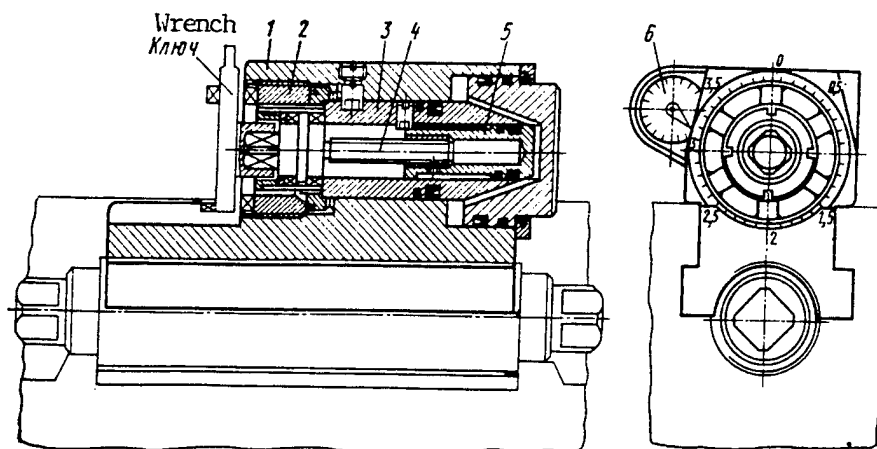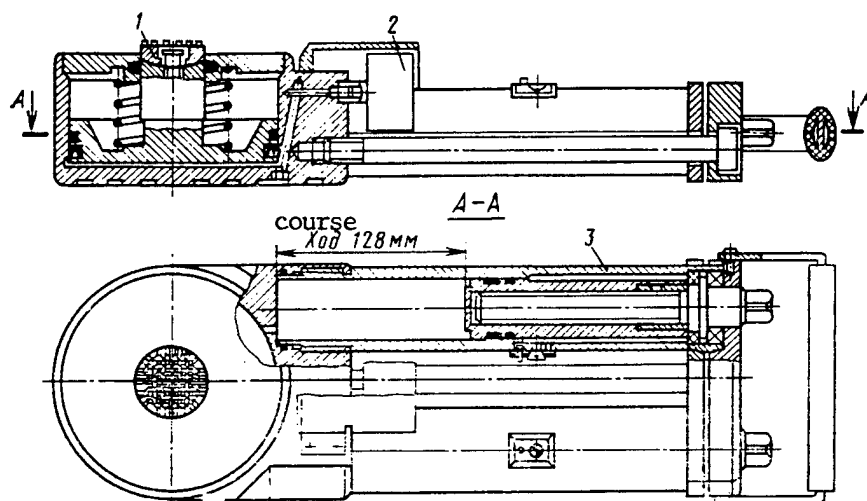
Figure 1

Figure 2

UDC 658.512.011.56;681.3.06;621.941.23-529

Using CAD for Technological Preparation of Production

18610396h Moscow MASHINOSTROITEL in Russian No 2, Feb 89 p 29

[Article by S. G. Stepanov, N. F. Kisenko, and Yu. I. Yefimenko, engineers]

[Text] The Donetskgormash Production Association and the Kramatorsk Machine Building Design, Planning, and Technology Institute have jointly introduced a system for the computer-aided design of control programs for type N122-1M NC lathes. It is geared toward a programmer-process engineer's workstation equipped with an Iskra-226 microcomputer.

The system has midlevel automation, i.e., the process engineer specifies a sequence of transfers that are automatically divided into passes. The source document for developing a control program is an operations sketch of the workpiece that has been developed in accordance with the shop drawing and production process route. Besides the geometry of the component that is required at the output of the specified operation, the operations sketch should also contain the dimensions of the blank, specifications of the cutting modes, and data about the sequence of machining by different tools.

the Iskra-226 microcomputer is designed for only one person to work on at a time. Designwise, it is in the form of a table-model central unit that contains a number of primary devices and that has a number of peripherals connected to it. Its components include the following: an interpreting interactive processor, a display with an external keyboard, hard and floppy disk storage units, a perforator, an alphanumeric printer, an optical scanner with punch tape, and a graph plotter.

When designing a control program on the computer, the programmer-process engineer works in an interactive mode. The external display keyboard is used to input source data from the operations sketch. The processor's output data are the formulated transitions of the lathe cycles in the form of records in the intermediate language CLDATA. The formulation of each pass is accompanied by a graphic image of the pass on the display screen. A postprocessor transforms data about a tool's motion into the codes of the specific NC system. The postprocessor's operation results in punch tape with a control program for an NC machine tool.

The system uses postprocessors for model 16K20F3S5, 16K30F325, 1B732F3, 1P732RF3, and RT720F305 machine tools that are equipped with one type N22-1M program control system. The system's software is implemented in the algorithm language BASIC.

The input language contains a dictionary of terms corresponding to generally accepted technological and design concepts that are used to specify the dimensions of a component's and a blank's surfaces and the other parameters of the cycle. The dialogue is designed in such a way that Yes or No answers or numbers corresponding to the size and technological information contained in the operations sketch of the component are sufficient to specify the source information. The correctness of the specification is checked when the geometric elements of a component and blank are calculated. The contour of a component of a blank is sketched on the display screen and may be copied on the graph plotter. The system's structure provides a block of utilities that may be used for online checking and editing of the control programs. The Service subroutines also take part in the man-machine interaction. At the end of an interaction about a component and blank, the interaction may be viewed on screen or printed out on paper; when necessary, it may be corrected.

After the data about the geometry of a component and blank have been specified, the stage of formulating the technological parameters of the machining process begins. During the course of this stage the cutting modes and tool parameters are determined. The trajectory of the cutting tool's motion is formulated and displayed on screen. If the process engineer is organizing a machining schematic, he selects the postprocessor that he needs and formulates the control program for a specific type of NC. If, for some reason, the machining schematic is not suitable, the technological information must either be respecified after restoring the geometry of the component and blank or else all the information must be specified again. The system makes it possible in each stage to correct the source data or to return to them for online respecification, thereby not allowing an erroneous control program. This approach to design reduces the time required to debug and test the control program.

The control program CAD system is designed on a multifunctional principle, i.e., it performs many tasks. The system makes it possible to input a program into the microcomputer's memory from punch tape while it reads an optical scanner or to enter a program manually from a panel, output frames of a program onto a display screen, find a specified frame when necessary, perform frame-by-frame program editing, implement graphic inspection of the trajectory being developed, perform various computations, search for subroutines, etc. An edited program may be placed into the computer's working memory or left in the RAM temporarily for output to punch tape, a printer, or a display. The system also makes it possible to norm the cycles of a control program being designed or of a previously developed control program.

Using a microcomputer that is located directly in a program preparation sector as an automated programmer-process engineer's workstation to design a control

program makes organizing the process of preparing programs for NC lathes both exact and quick. Compared with manual development, the labor intensity of thus preparing a control program has been reduced 60 to 70 percent, and the quality of the programs has been stabilized.

A second direction in using CAD, i.e., performing applied engineering tasks at an Iskra-226 programmer-process engineer's workstation, entails labor-intensive technical calculations. This direction was developed with regard to tooth-cutting machine tools by specialists from the department of the association's chief technologist. The required volume of algorithms have been determined, and the calculations have been performed: the worm mill angles for setting up model 3662 and KARR tool-grinding machines, the loads of auxiliary workers involved in the electroerosion hardening of a cutting tool, and the cutting modes and production time required for grinding the teeth of the components' representative reducing gears.

Using a programmer-process engineer's workstation to calculate the data needed to set up gear-cutting machines for cutting bevel gearings with a round even-height tooth is a labor-intensive task during manual design. The program developed for the Iskra-226 makes it possible to produce a finished chart of set-up data for the tooth-cutting production process on an alphanumeric printer. The program is based on a method of setting up tooth-cutting machines that is in turn based on strict analytical dependencies ensuring the constancy of the instantaneous gear ratio of the pair being cut. This excludes the possibility of the contact spot being diagonal when inserted blade milling cutters are used simultaneously. This work is done interactively on a microcomputer. The user inputs source data from a terminal by using only a sketch of the bevel gearing and a table to select the change gears. It takes 5 to 10 minutes to develop one set-up chart, and the calculations are highly exact and correct. Automating this task makes it possible to correct the compatibility of teeth quickly and precisely so as to achieve optimum contact in a bevel gearing, i.e., to synthesize conical gearings.

©Izdatelstvo "Mashinostroyeniye", Mashinostroitel, 1989

658.52.011.56.012.3;658.310.8

Determining Number of Personnel Required for FMS

18610396i Moscow MASHINOSTROITEL in Russian No 2, Feb 89 pp 39-40

[Article by A. N. Kolosov, candidate of economic sciences]

[Text] Because the organization of service for automated equipment is fundamentally different than in traditional production systems, it requires new methods of establishing the number of service personnel that are specific

for flexible manufacturing systems [FMS]. A step-by-step refinement of the makeup and numbers of the personnel for an FMS was tested during the development of a number of machining flexible manufacturing complexes. The occupational makeup and numbers of personnel in an FMS are determined by considering the makeup of the functional components of the FMS, the structure of the production cycle of the product's manufacture, labor expenditure norms for performing service operations, and norms regarding the numbers of individual categories of service personnel (engineering and technical personnel, mathematicians and programmers, repairers, etc.).

The list of duties of engineering-technical and administrative personnel is established in accordance with the production structure and management system of FMS. The number of personnel by specified category is determined with an allowance for existing recommendations (MASHINOSTROITEL, No 11, 1987, p 26).

The number of personnel is calculated on the basis of normed operations in the following sequence: the initial list of occupations and duties of the workers in each category per one standard cycle in the product's machining is determined; a preliminary estimate is made of the number of workers in each category; and the number of personnel for the FMS is determined in light of the yearly volume of work performed, the combining of occupations, and the operating mode by shift.

The number of machine building by specified category (P_{0i}) is preliminarily determined by the formula

$$P_{0i} = t_{0i}R/t_{com\ i},$$

where t_{0i} is the time for which workers belonging to the i-th category are occupied (calculated for one cycle of single-operation machining), R is the amount of equipment in the FMS, and $t_{com\ i}$ is the period of a complete cycle of servicing a specified type of equipment (in the general case, it is the period during which service of one object is received).

The period of the arrival of requests differs for different categories. Thus, when products are machined in a single operation, the average period during which requests for adjusters are received is specified in terms of the average interval of the receipt of orders to machine batches of products in the FMS $t_{ord} = F_{real}/N$, where F_{real} is the annual actual fund of working time in the FMS and N is the yearly quantity of batches of products machined.

In the case of multioperation machining, the average interval of the arrival of requests to adjust each machine tool is specified in terms of the average duration of a machining operation $t_{mac} = t_{unit}p$, where t_{unit} is the average unit time required to machine products in one operation and p is the size of the transport batch.

For tool adjusters, the period for which requests arrive is, on average, characterized by the durability of the tool setups, which is determined on the basis of the limiting tool. For operator-controllers, the request period is specified as the duration of the machining cycle because the set of jobs performed by an operator is related to the maintenance of each transport batch. In the case of operations that take a long time to implement, for example, when machining housing components on universal machine tools (machining centers) where the unit time ranges from 2 to 4 hours, it is possible to establish the interval for an operator as that interval during which

he makes one approach to the working equipment and the time spent on this, depending on the functions being performed.

Preliminary calculations based on the formula presented above demonstrate the single-moment apparent number in a cross section of the single-shift operation of the FMS and are subject to further refinement.

Table 1 presents an example of the preliminary determination of the number of individual categories of personnel for an FMS for machining components (bodies of revolution, for example).

Table 1

Category of Personnel	No. Machine Tools	Time Occupied, h	Time for Which Blanks Arrive From One Machine Tool	No.
Equipment adjuster	8	0.53	10.24	0.41
Tool adjuster	8	0.25	2.88	0.54
Operator-controller	8	0.82	4.64	1.4

As is evident from the table, calculations of the single-moment population of the FMS are not very simply matched with the real labor process of laborors in view of the requirements of their total number, their number relative to the full load, or the evenness of the distribution of the worker population in accordance with labor legislation, etc.

A refined calculation of the shift population of workers in each category in accordance with the yearly volume of work performed may be made in accordance with the formula

$$P_i = t_{occ}B_y/\Phi_{rf}k_{shw}k_{nocc},$$

where t_{occ} is the time for which a worker is occupied (calculated for one standard cycle), in hours; B_y is the yearly number of cycles (component batches, operations, tool setups, or transport batches) implemented; Φ_{rf} is the real working time fund, in hours; k_{shw} is the shift employment coefficient of the workers comprising the personnel of the FMS; and k_{nocc} is the admissible norm coefficient, which is established in accordance with recommendations by the Labor Scientific Research Institute as between 0.75 and 0.95.

We will illustrate the preliminary calculations of the apparent number of certain categories of personnel in an FMS for machining housing components and its refinement in view of all of the factors entailed in organizing the labor process.

The number of operator-controllers is calculated with an allowance for their employment in servicing four machining centers. The time for which the operation of

one machine tool is actively observed is estimated such that a worker approaches a machine tool once every hour and a half. The time for which an operator is occupied, including moving from one workstation to another, visual monitoring, and making measurements, amounts to 9 minutes. The request period thus amounts to 0.5 hours, and the apparent number of operators P_{op} amounts to 9 time 4 divided by 30 or 1.2 persons. FMS operate in three shifts with an equipment shift coefficient $k_{sh\ eq}$ of 2.55, which means an effective yearly equipment operating fund of 5,200 hours and 2,040 hours per full shift. Since the real yearly shift time fund for a worker is less (Φ_{rf} = 1,840 hours), the worker shift coefficient $k_{sh\ w} = k_{sh\ eq}$ x 2,040/1,840 = 2.83. The total required apparent number of operators comes to 1.2 x 2.83 = 3.4 persons.

The source data for determining the number of tool adjusters is the average time required for assembly/disassembly, the durability of the tool setups, and the yearly number of batches put into production.

The required number of tool adjusters P_{adj} is determined with an allowance for the multishift operation of the FMS in accordance with the formula

$$P_t = t_tN_{com}/\Phi_{rf}n_tk_{shw},$$

where t_t is the average time required to assemble/disassemble one tool setup (0.72 hours), N_{com} is the yearly number of components machined (33,187 units), Φ_{rf} is the real yearly working time fund of a worker (1,840 hours), and n_t is the average number of components machined with one tool setup.

The average number of components machined with one tool setup is determined in accordance with the formula

$$n_t = AN_t/t_u k_{main} = 60 \times 12/40.8 \times 0.75 = 24 \text{ components,}$$

where A is the average durability of the cutting tool in a tool setup (60 minutes), N_t is the average number of cutting tools in a tool setup (12 units), t_u is the time required for the online machining of one component from one setup (in minutes), and $k_{main} = 0.75$ is the coefficient characterizing the ratio of the machine time to the online time. Then,

$$P_t = 0.72 \times 33,187/1,840 \times 24 \times 2.83 = 0.20 \text{ persons.}$$

The total apparent number of tool adjusters is, in this case, equal to 0.2 x 2.83 = 0.57 persons.

The required number of pallet assemblers is determined with an allowance for the labor intensity of assembling the attachment, configuring it on a change satellite table, and mounting components on it, which, when combined with the various setup and finishing operations, amounts to 36 minutes.

The required number of component assembly workers P_{as} per shift is calculated in accordance with the formula

$$P_{as} = N_{com} t_{as}/\Phi_{rf} k_{shw} 60 = 33,187 \times 36/1,840 \times 2.83 \times 60 = 3.82 \text{ persons,}$$

where N_{com} is the yearly number of components and t_{as} is the time for which an assembly worker is busy (36 minutes). The total number of assembly workers needed amounts to 3.82 x 2.83 = 10.8 persons.

The number of workers involved in servicing the FMS equipment between repairs is calculated on the basis of norms for repairs on machine tools with program control that are performed by an operator, shift mechanic, electrician, or electronics specialist. The source data for the calculation are as follows:

no. pieces of equipment (four model 66K12F4 NC machine tools, one stock-piling robot, and one tool-worker-robot);

indicators of the complexity of repairing the equipment being serviced;

the mechanical and hydraulic part $R_m = 51 \times 4 + 15 \times 1 + 13 \times 1 = 232$ repair units;

the electrical engineering part $R_{el} = 56 \times 4 + 18 \times 1 + 17 \times 1 = 259$ repair units;

the electronic part $R_{elec} = 55 \times 4 + 55 \times 1 + 55 \times 1 = 330$ repair units;

the machine shift coefficient (2.4);

norms for between-repair service for one worker per shift:

for the mechanical and hydraulic part $N_m = 380$ repair units;

for the electrical engineering part $N_{el} = 450$ repair units;

for the electronic part $N_{elec} = 450$ repair units.

The number of workers required per shift to service program control machine tools between repairs is determined by the formula

$$P_{rep} = \Sigma W/N_0,$$

where ΣW is the total number of repair complexity units based on the component parts of the equipment being serviced and N_0 is the service norm for one worker per shift (the number of repair units). As a result, the estimated number of mechanics amounts to 232/380= 0.61, the number of electricians comes to 259/450 = 0.57, and the number of electronics specialists comes to 330/450 = 0.73. Accordingly, the following numbers of workers are required for a full workday: 1.73 mechanics, 1.61 electricians, and 2.06 electronics specialists.

Table 2 has been compiled on the basis of estimates of the number of service personnel by category.

Table 2

Category of Service Personnel	No. Persons per Shift	No. Persons per Day*
Tool adjuster	0.20	0.57
Operator-controller	1.20	3.4
Component assembler	3.82	10.8
Mechanic for service between repairs	0.61	1.73
Electrician for service between repairs	0.57	1.61
Electronics specialist	0.73	2.06
Apparent no.	7.13	20.17

* $k_{shifts \times workers} = 2.83$)

Table 3 demonstrates the determination of the actual apparent number of workers in the FMS and their distribution in the FMS by shift.

Table 3

Category of Workers	Estimated Apparent No.		Assumed Actual No.	Actual Distribution of No. by Shift		
	Per Shift	Total		1	2	3
Tool adjuster	0.2	0.57	-	1.33	1.33	1.33
Operator-controller	1.2	3.4	4*	3.67	3.67	3.67
Component assembler	3.8	10.8	11	1.33	1.33	1.33
Mechanic for service between repairs	0.61	1.73	4**			
Electrician	0.57	1.61	-	0.67	0.67	0.67
Electronics specialist	0.73	2.06	2			
Total	7.13	20.17				

*The occupations of tool adjuster and tool operator are combined;
**The occupations of mechanic and electrician are combined.

A balance is achieved between the estimated and actual numbers by combining the occupations of tool adjuster and operator-controller as well as by using a sliding graph of workers' output by shift.